Particle acceleration in SNRs
—Origin of Galactic cosmic rays

Siming Liu, Houdun Zeng, Yiran Zhang, Zhaodong Shi, Yuliang Xin, Qiang Yuan

Purple Mountain Observatory

LHAASO， 林芝

Outline

- Background
- Evolution of high-energy particle distribution in SNRs
- Cosmic ray electrons and positrons
- Conclusions

Background

Supernova remnants (SNRs) have been proposed as the dominant contributors to galactic cosmic rays (Baade & Zwicky 1934).

1、SNRs have enough total power —3 SNRs per century with a 1e51erg shock kinetic energy for each SNR, a 10% efficiency leads to the observed CR density (1ev/cm3)；

2、 Direct evidence:

Radio emission (1948)
— GeV electrons

Non-thermal X-ray emission (1995)
— TeV electrons

π^0 bump (2013)W44,IC443,W51C
— GeV protons

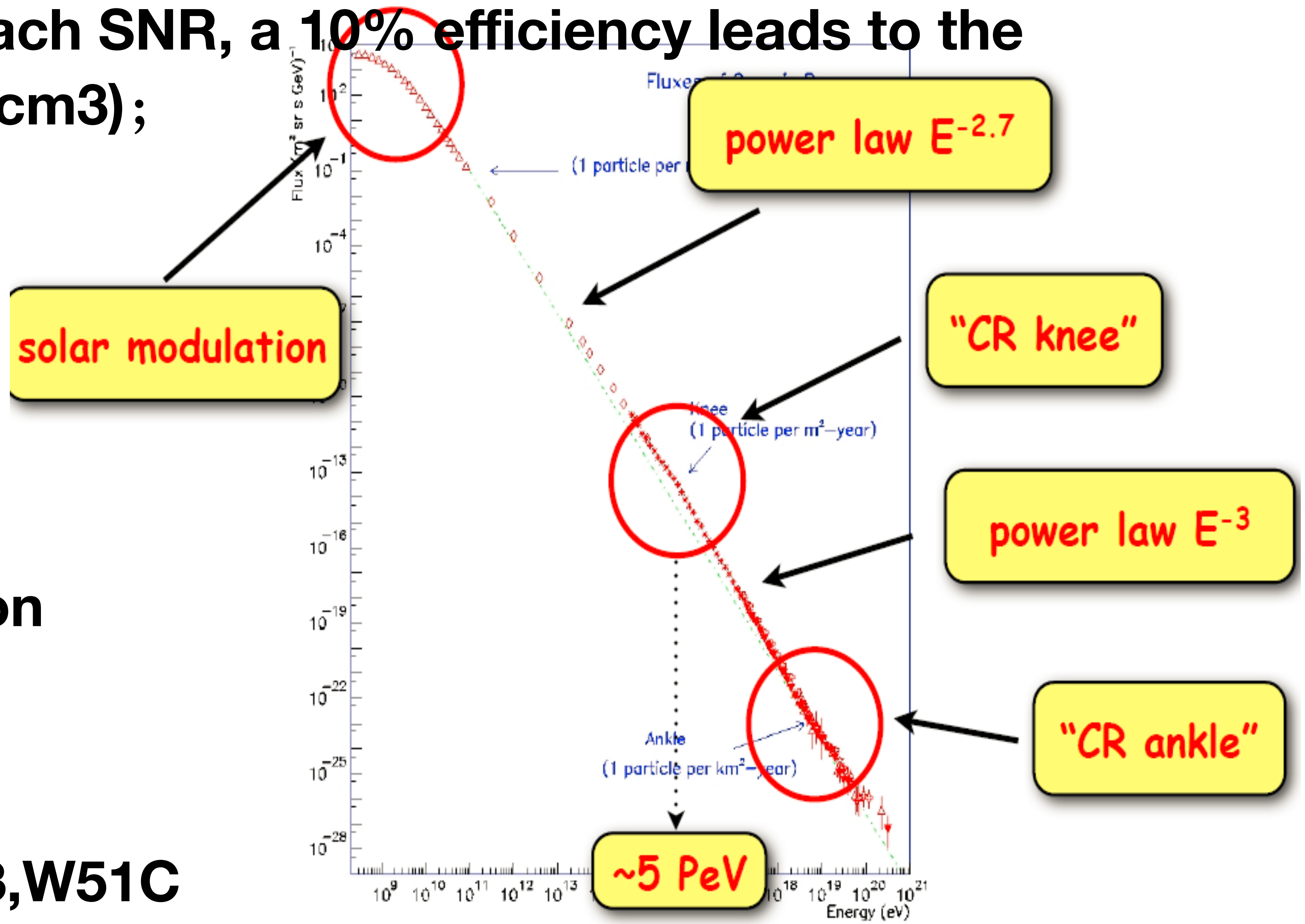

Background

中国科学院紫金山天文台

standard theory of shock predicts p=2.0

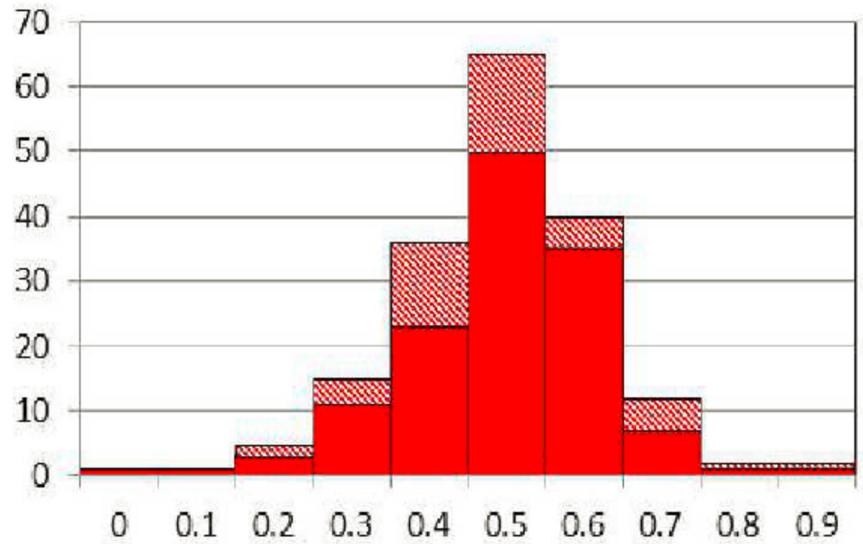

Fig. 6 Histogram of spectral indices of shell-type Galactic SNRs as extracted from Green (2014). The solid bars correspond to firm spectral index determination, while the shadowed ones to SNRs with uncertain spectral indices

Relation?

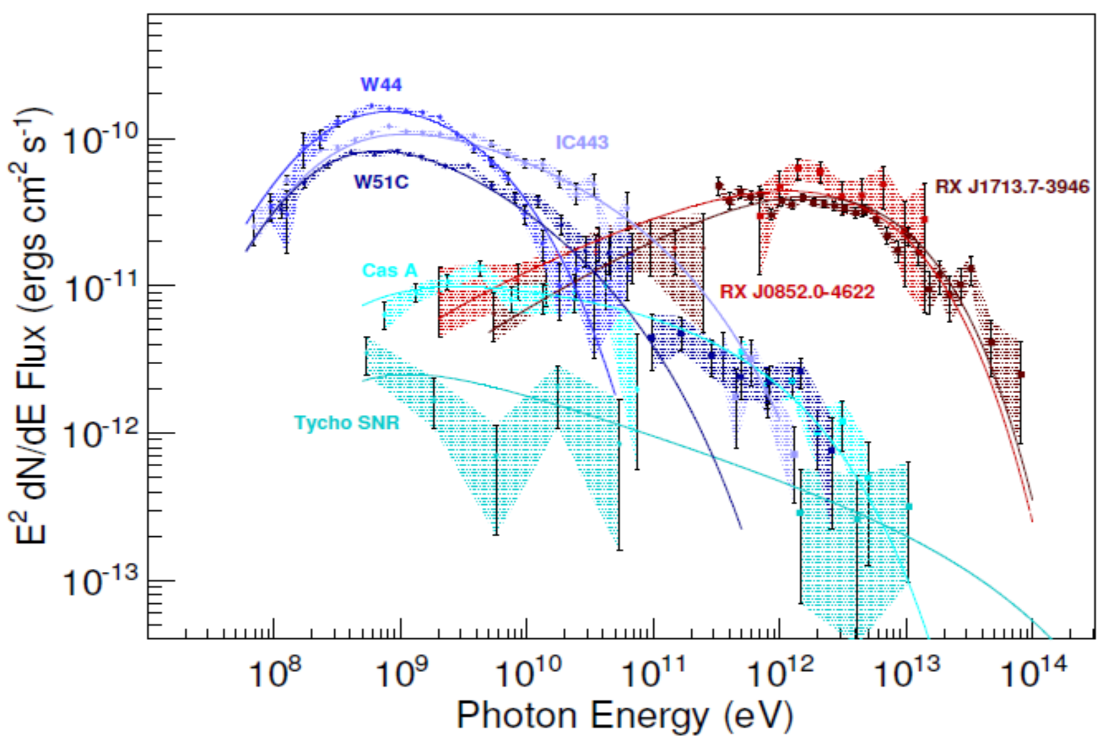

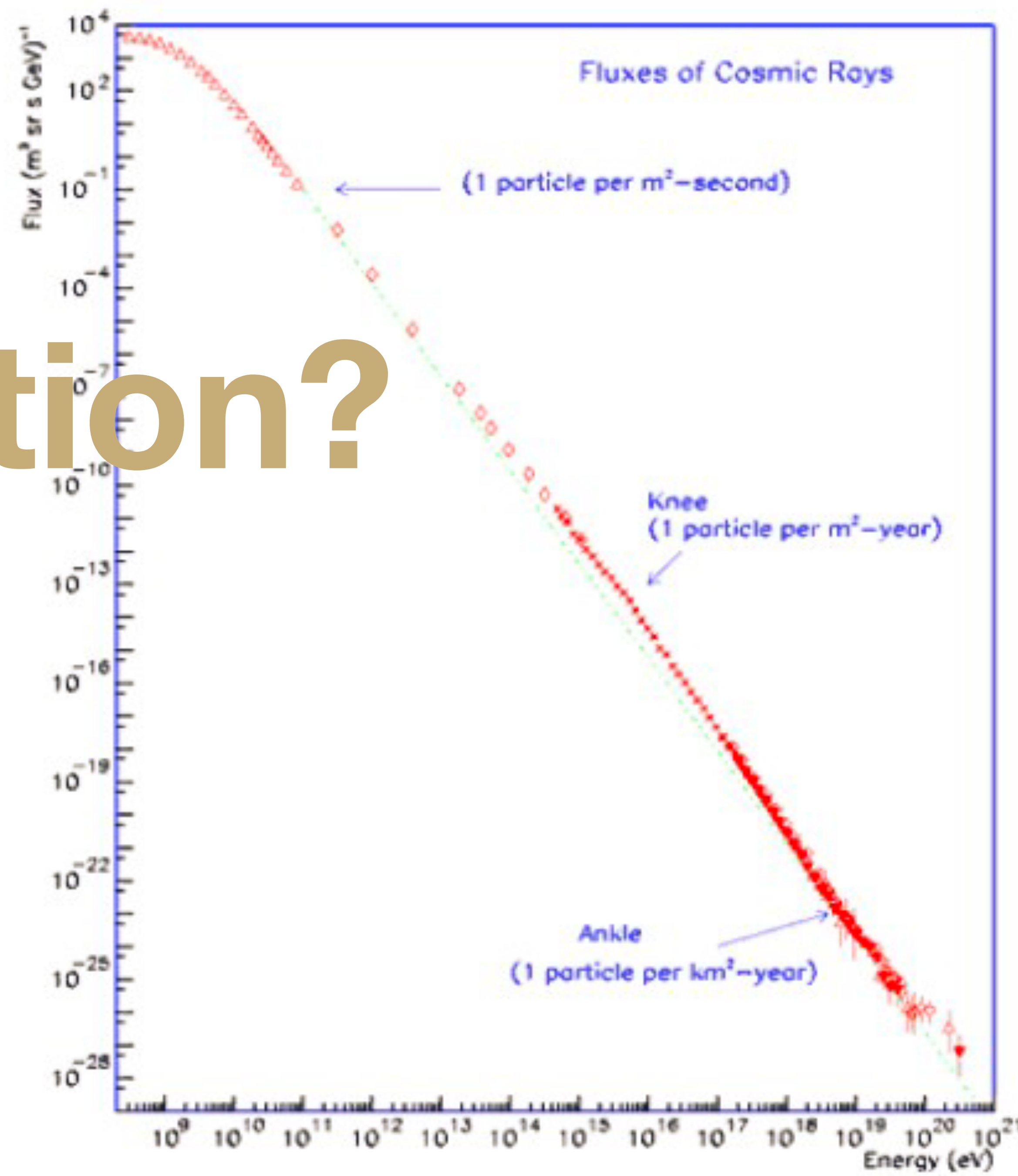

Background

$$q_f(R,z) \propto \left(\frac{R}{R_\odot}\right)^\alpha \exp\left[-\frac{\beta(R-R_\odot)}{R_\odot}\right] \exp\left(-\frac{|z|}{z_s}\right),$$

$$q(p) \propto \begin{cases} p^{-\alpha_1}, & p < p_{\rm br}, \\ p^{-\alpha_2}, & p \geq p_{\rm br}, \end{cases}$$

$p_{\rm br}c = 6$ GeV

$\alpha_1 = 1.80, \ \alpha_2 = 2.52$

Injection Power :
Proton ~ 3e48 erg/year
Electron ~ 4e46 erg/year

3 SNRs/100 yrs with
1e50 erg protons and
1e48 erg electrons
For each SNR.

10% efficiency for type
Ia SNRs with a kinetic
energy of 1e51ergs

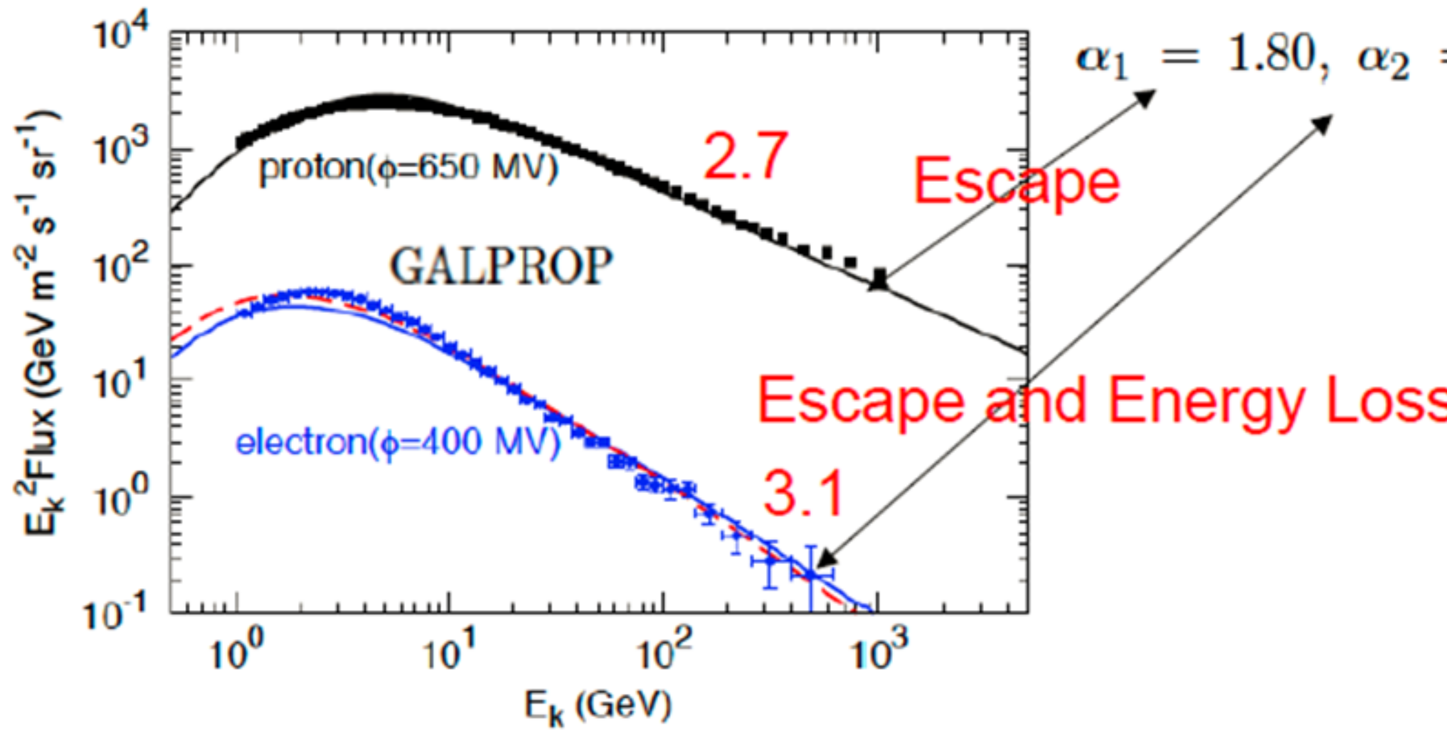

FIG. 1.— The expected fluxes of CR protons and electrons at the Earth, for the same spectral shape of the injected particles, compared with the PAMELA observational data (Adriani et al. 2011a,b). We adopt two parameter settings to calculate the electron spectrum: for solid line the magnetic field is the canonical one adopted in GALPROP and $K_{ep} \approx 1.3\%$; for dashed line the magnetic field is two times larger and $K_{ep} \approx 1.9\%$.

Yuan et al. 2012

Background

THE ASTROPHYSICAL JOURNAL LETTERS, 844:L3 (5pp), 2017 July 20
https://doi.org/10.3847/2041-8213/aa7de1

CrossMark

中国科学院紫金山天文台
PURPLE MOUNTAIN OBSERVATORY, CAS

Anomalous Distributions of Primary Cosmic Rays as Evidence for Time-dependent Particle Acceleration in Supernova Remnants

Yiran Zhang[1,2], Siming Liu[1,2], and Qiang Yuan[1,2]
[1] Key Laboratory of Dark Matter and Space Astronomy, Purple Mountain Observatory, Chinese Academy of Sciences, Nanjing 210008, China

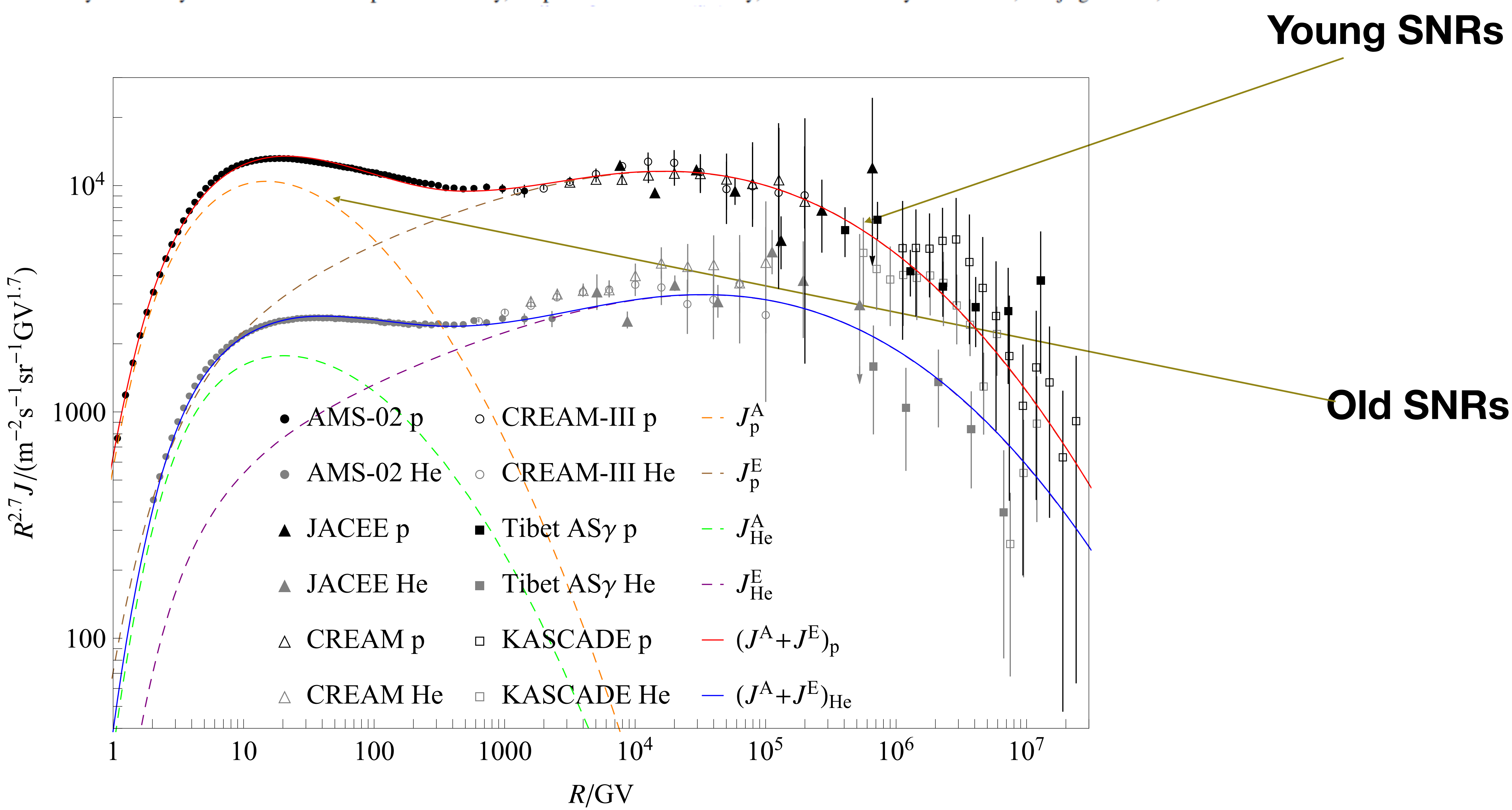

Background

n=0.01

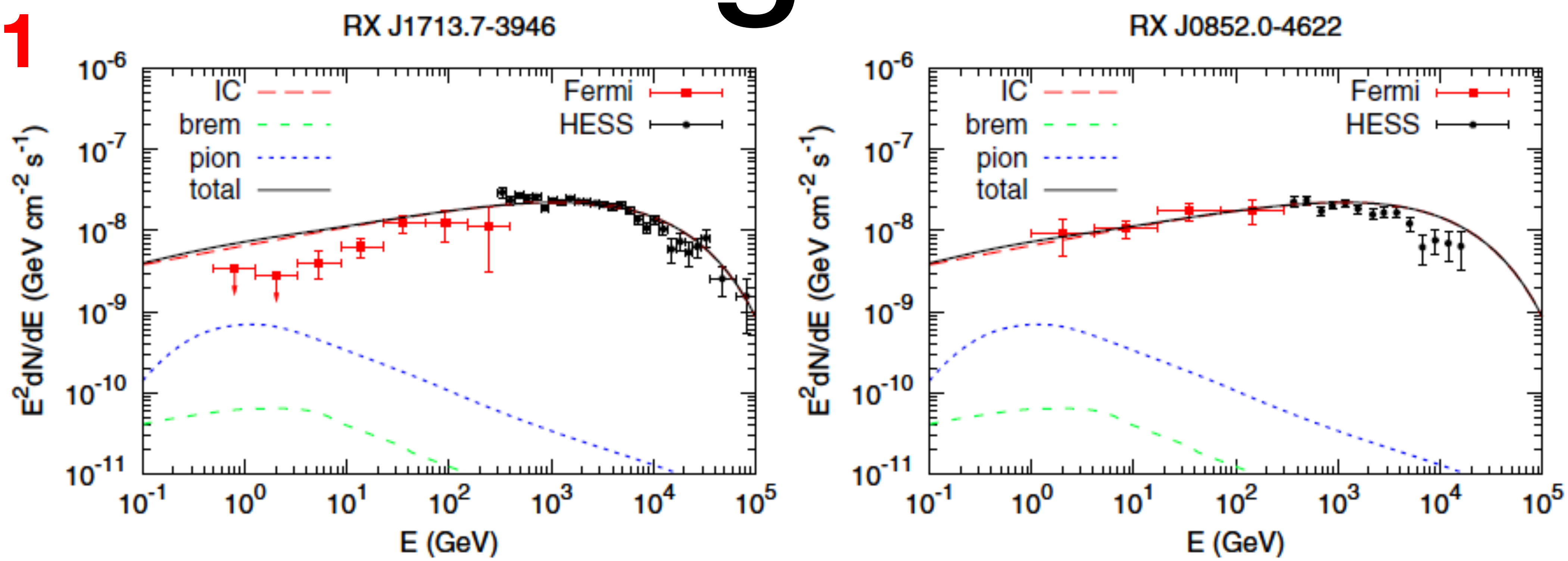

Figure 2. Expected γ-ray spectra for SNRs RX J1713.7−3946 (left) and RX J0852.0−4622 (right). The gas density is adopted to be $n = 0.01\ \mathrm{cm}^{-3}$. References of the observational data—RX J1713.7−3946: *Fermi* (Abdo et al. 2011), HESS (Aharonian et al. 2007b); RX J0852.0−4622: *Fermi* (Tanaka et al. 2011), HESS (Aharonian et al. 2007a).

n=1.0

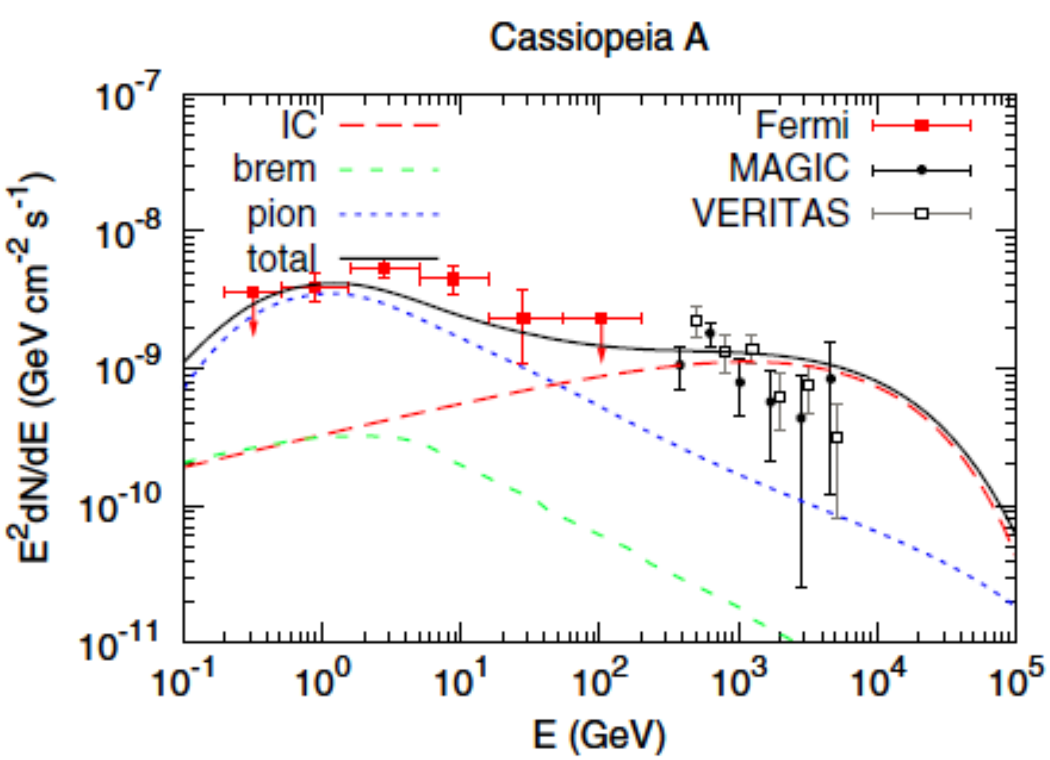

n=100

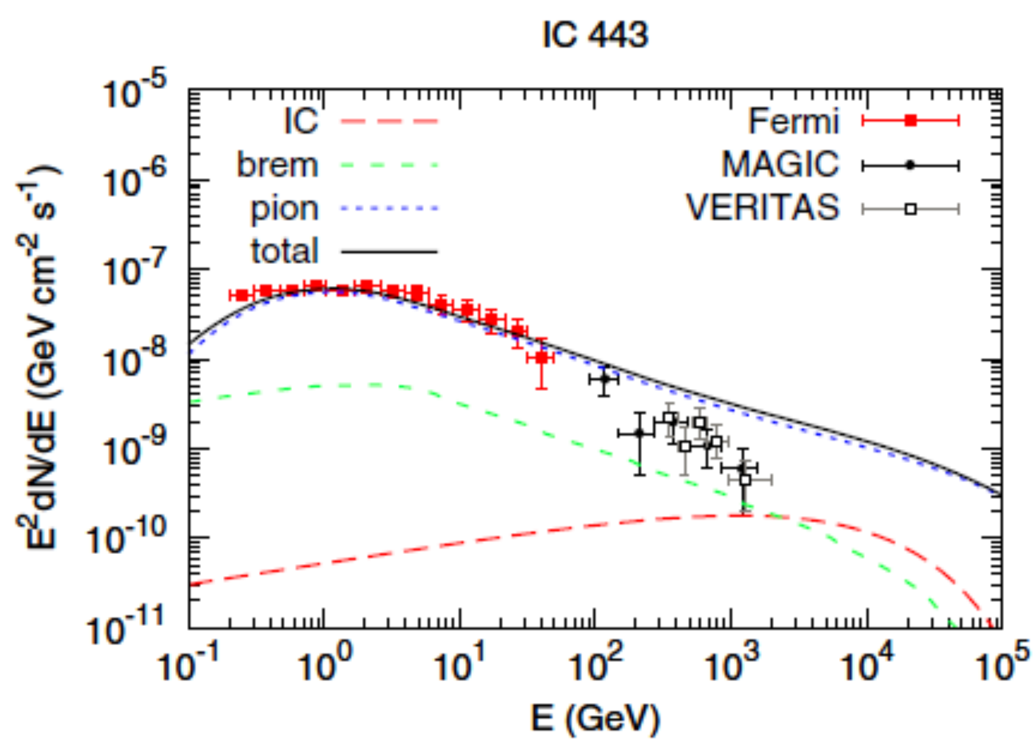

Gamma-ray spectral evolution

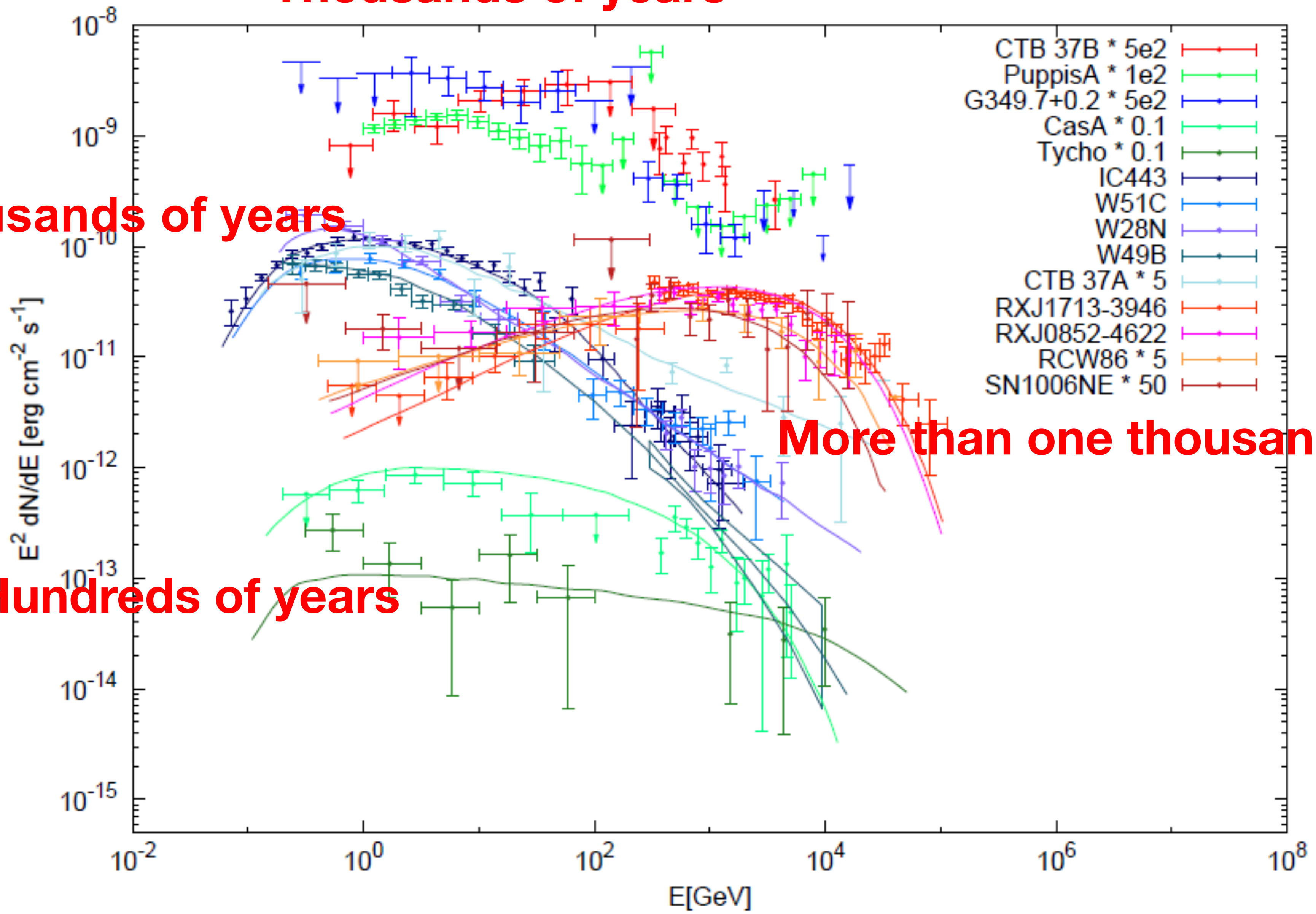

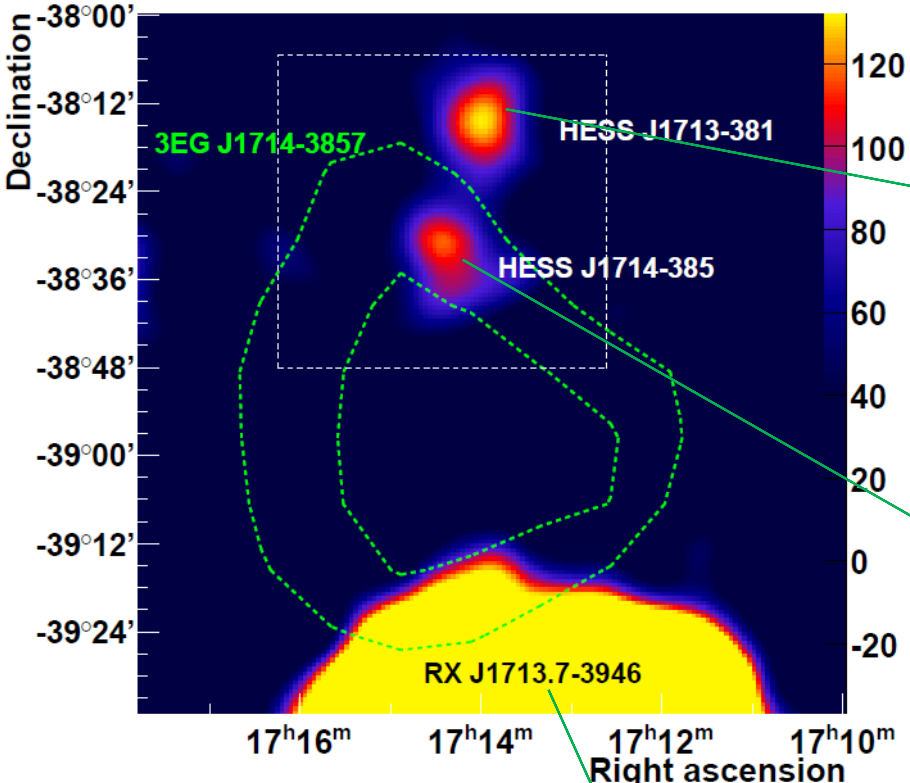

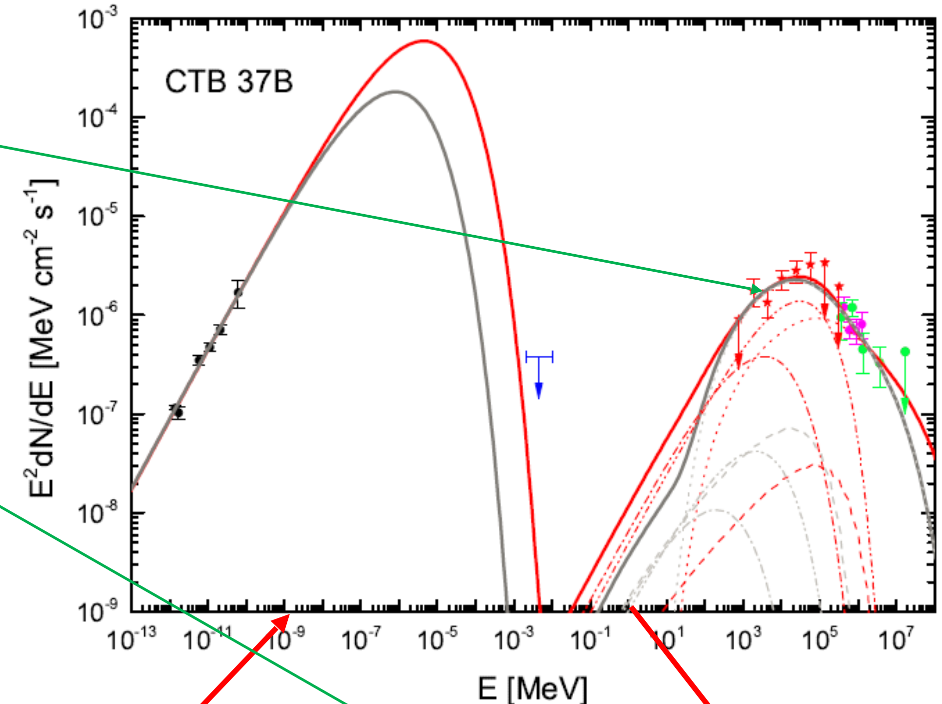

CTB 37B:
~5000 Years
Ebr~400GeV
Both IC and pp contribute to γ-rays

CTB 37A:
>10000 Years
Ebr~2GeV
pp dominates γ-rays

RX J1713.7-3946
1600 Years Ebr~1TeV
IC dominates γ-rays

The evolution of SNRs' SEDs

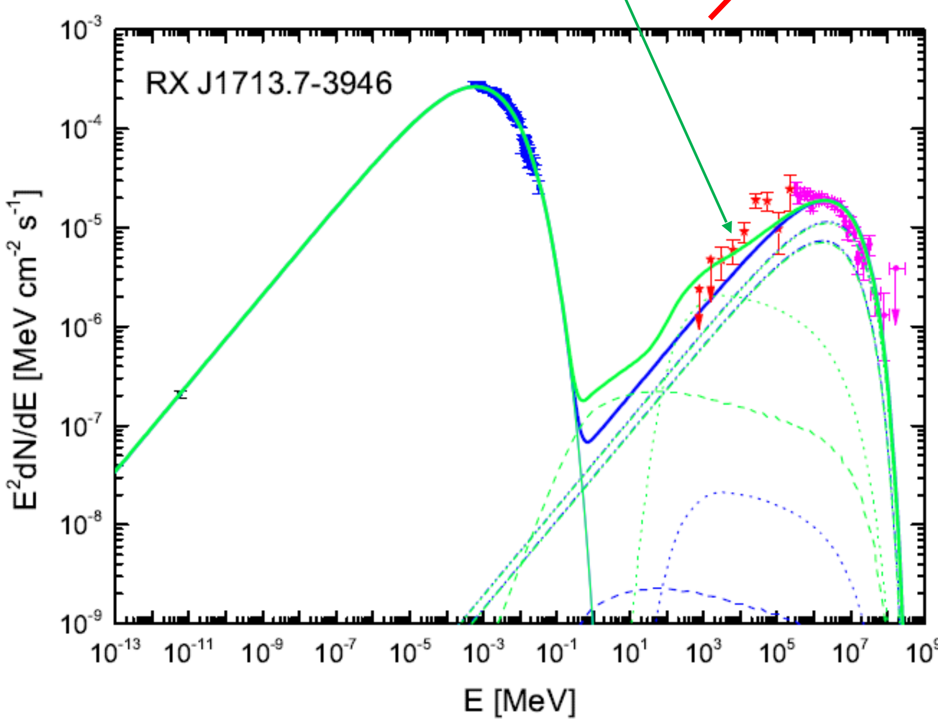

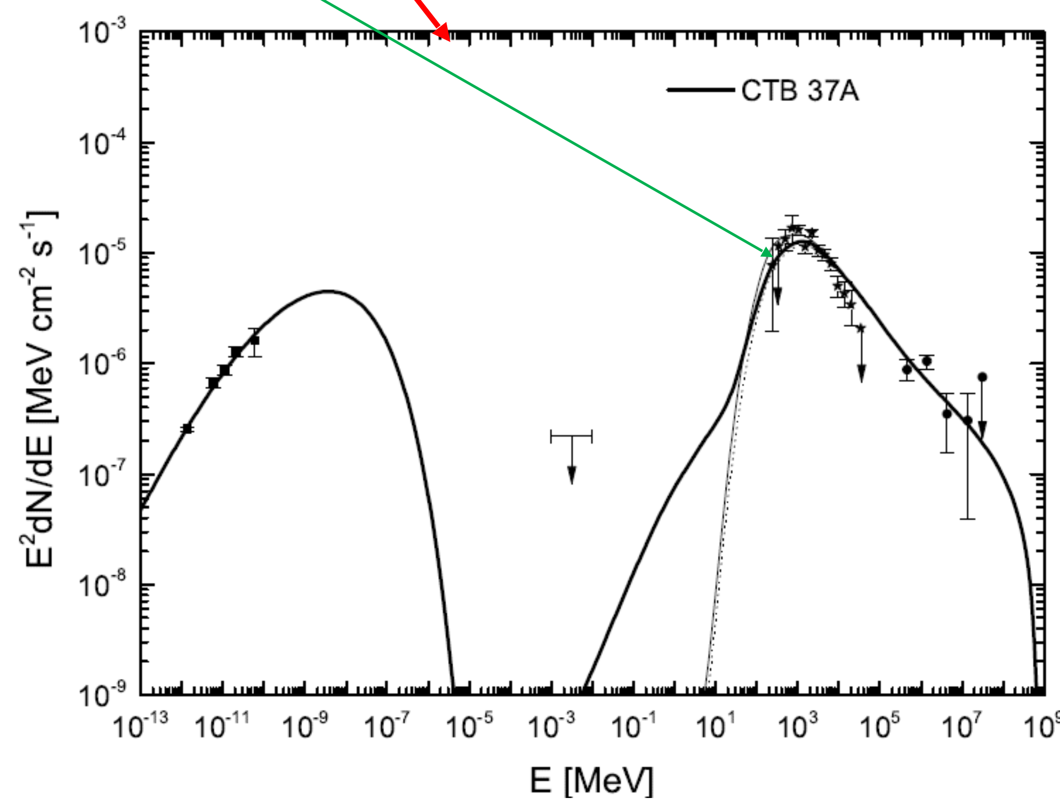

Zeng, H. et al. 2017, ApJ, 834, 153

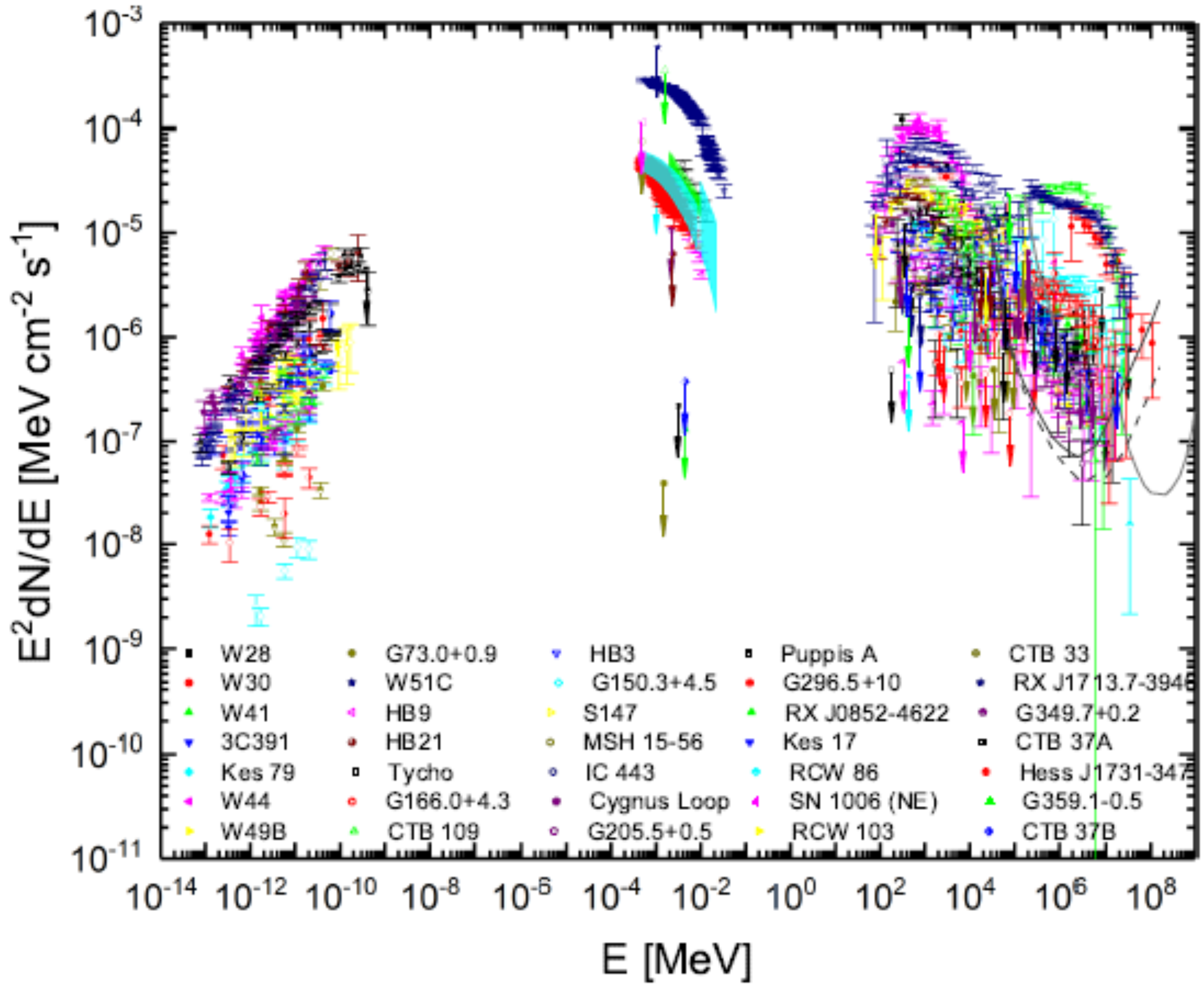

34 SNRs have been selected, 6 X-ray, 16 TeV data

We normalize the flux at100 GeV to 1 x 10^{-5} MeV cm^{-2} s^{-1} by a power-law fit to the spectrum from 1 GeV to 300 GeV to better demonstrate the spectral evolution.

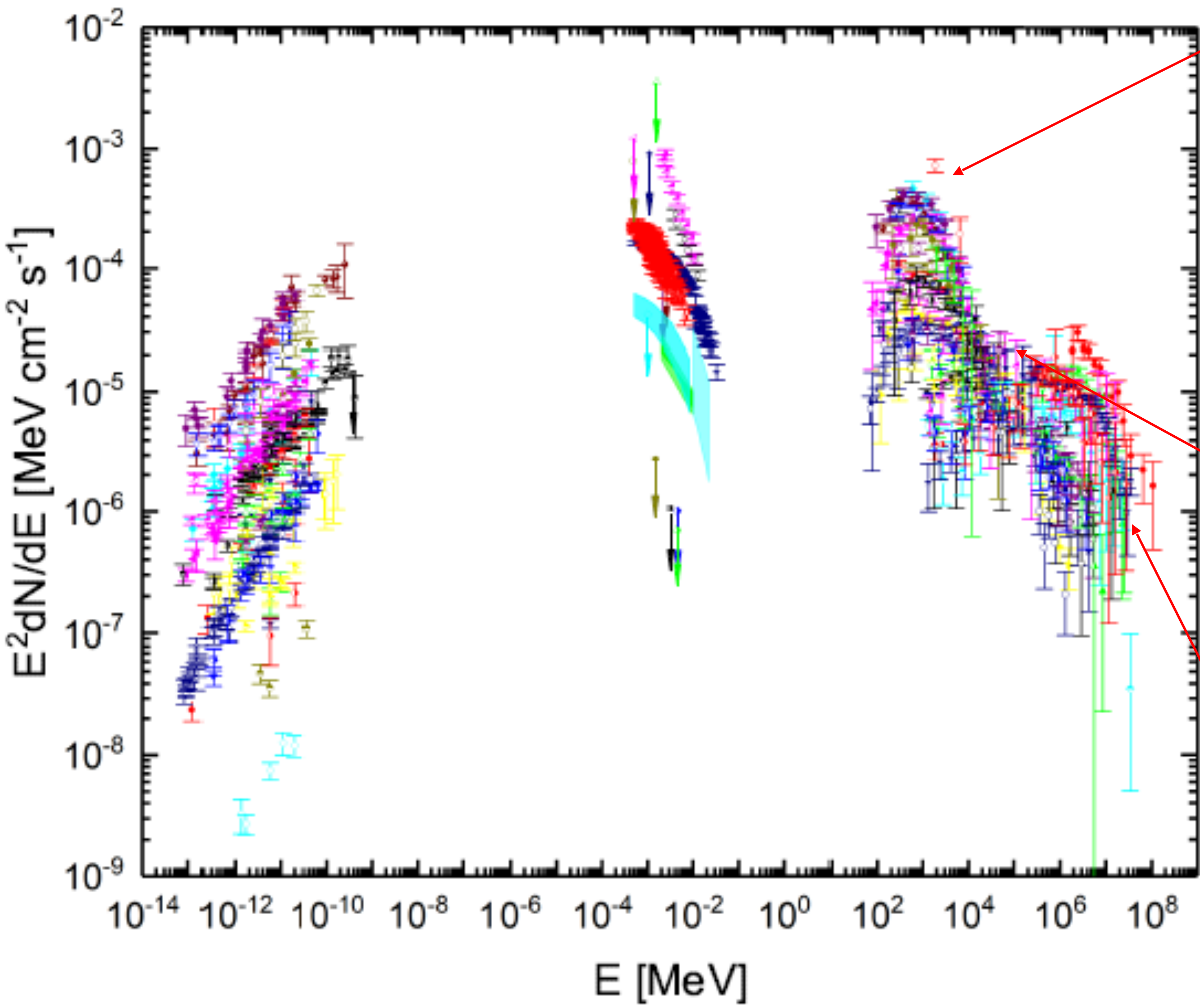

Break energy

1-20GeV:

W28 (Abdo et al. 2010a),
W51C (Abdo et al. 2009; Aleksic et al. 2012), W49B (Abdo et al. 2010c; Brun et al. 2011), IC 443(Acciari et al. 2009; Ackermann et al. 2013)
W41 (Aharonian et al. 2006b; Castro et al. 2013) and so.

20-200GeV:

G349.7+0.2(Hess Collaboration et al. 2015), CTB 37B(Xin et al.2016), Puppis A (Xin et al. 2017)

1TeV:

RX J1713.7-3946(Hess Collaboration et al. 2017)

A model for broken power-laws in SNRs

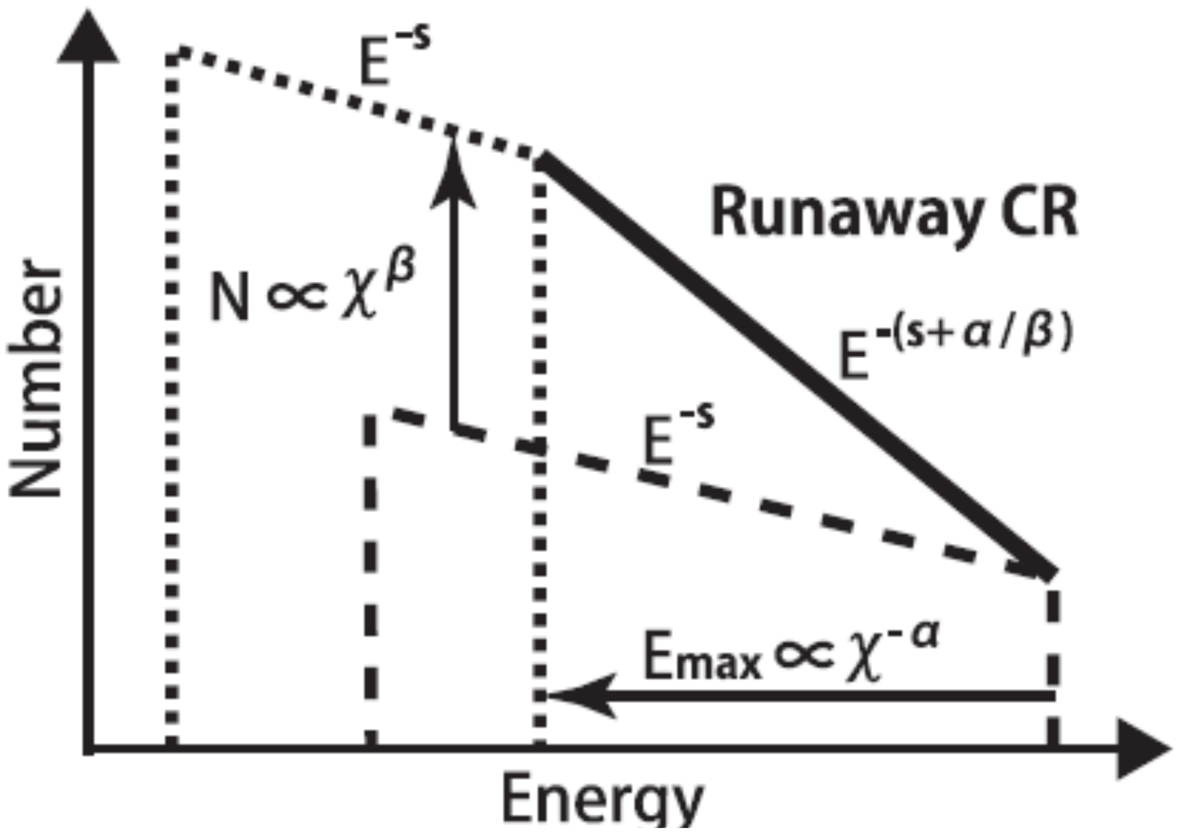

THE ASTROPHYSICAL JOURNAL LETTERS, 729:L13 (5pp), 2011 March 1

COSMIC-RAY HELIUM HARDENING

YUTAKA OHIRA AND KUNIHITO IOKA

Mon. Not. R. Astron. Soc. **427,** 91–102 (2012) doi:10.1111/j.

Escape of cosmic-ray electrons from supernova remnants

Yutaka Ohira,[1★] Ryo Yamazaki,[1] Norita Kawanaka[2] and Kunihito Ioka[3,4]

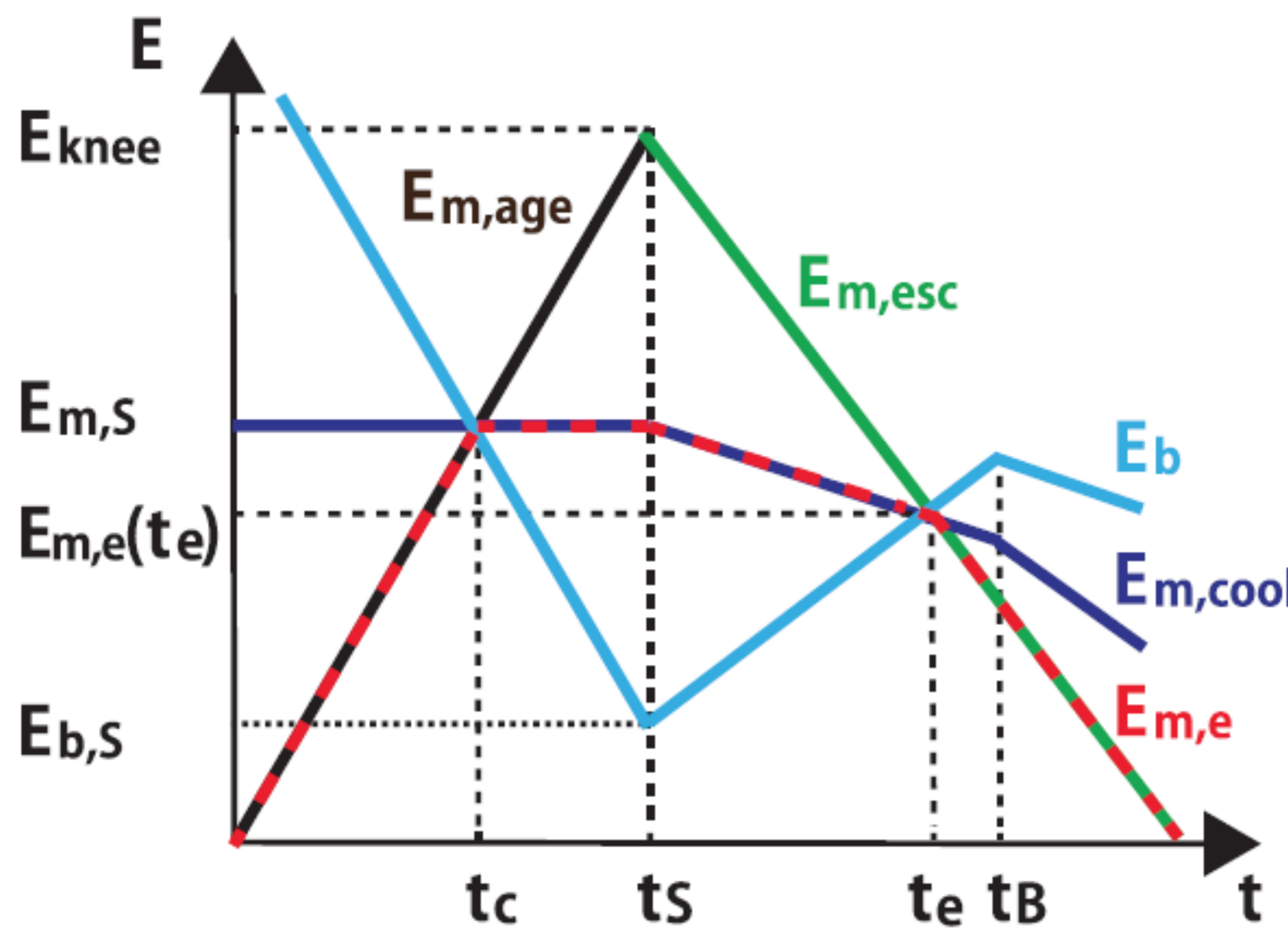

Hα observations

Tycho

Young with wider precursor for higher energy acceleration

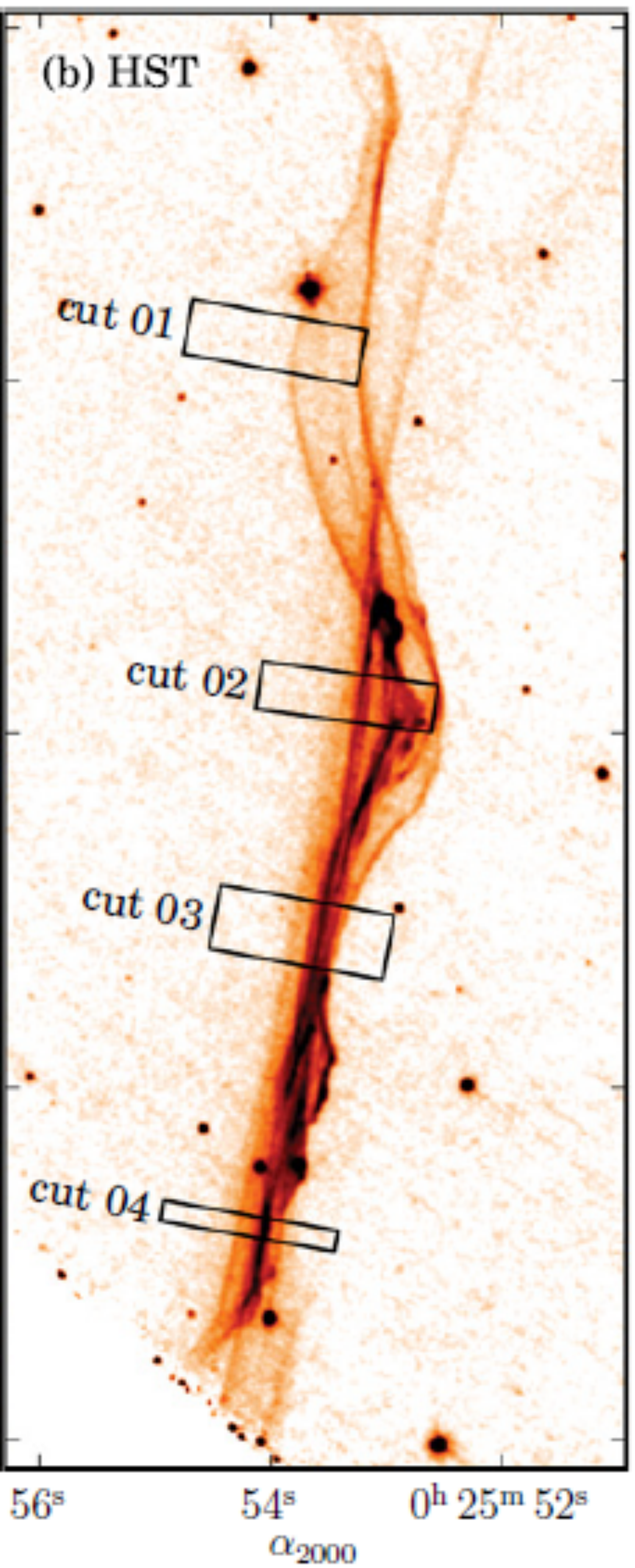

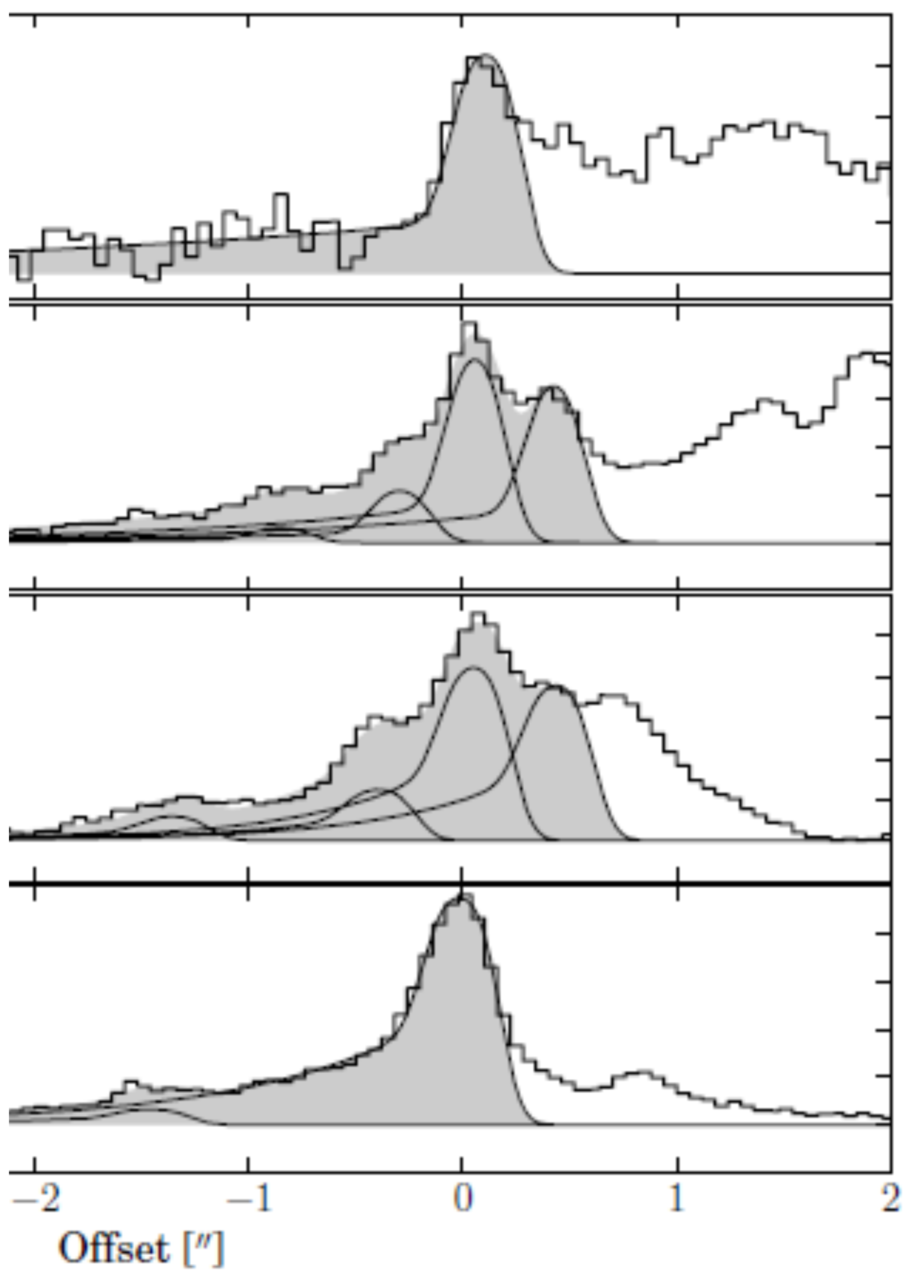

Cygnus loop old

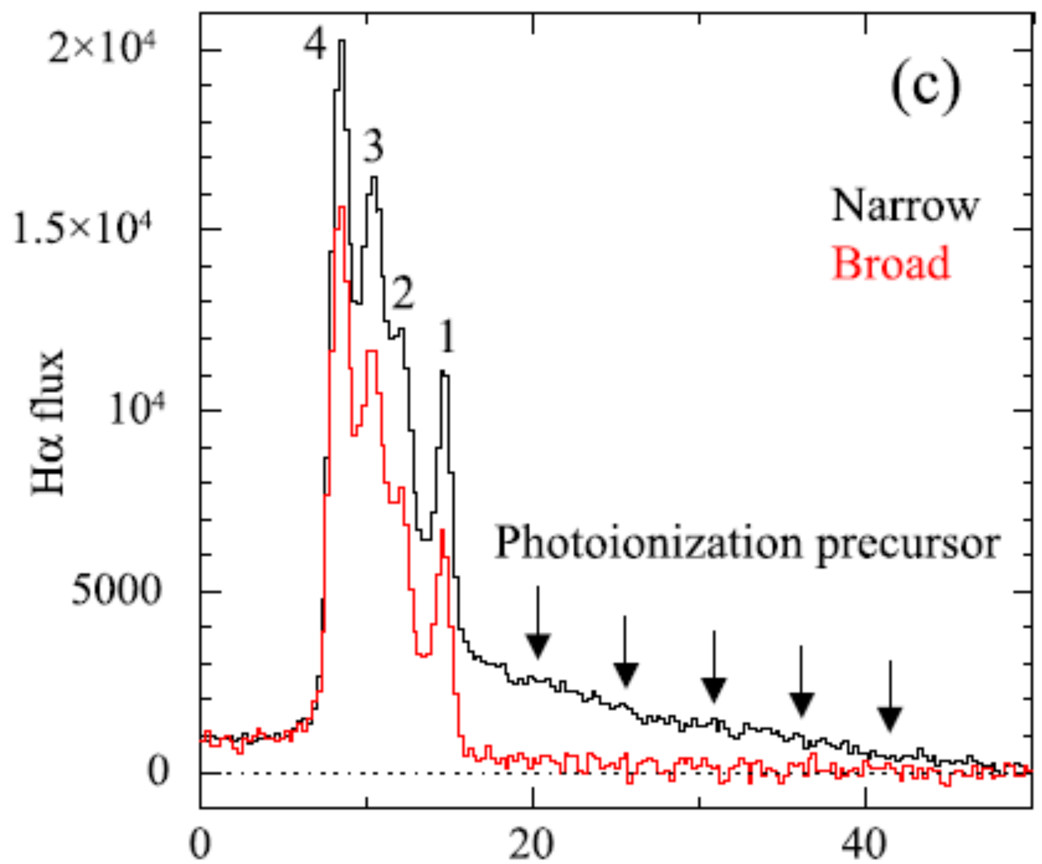

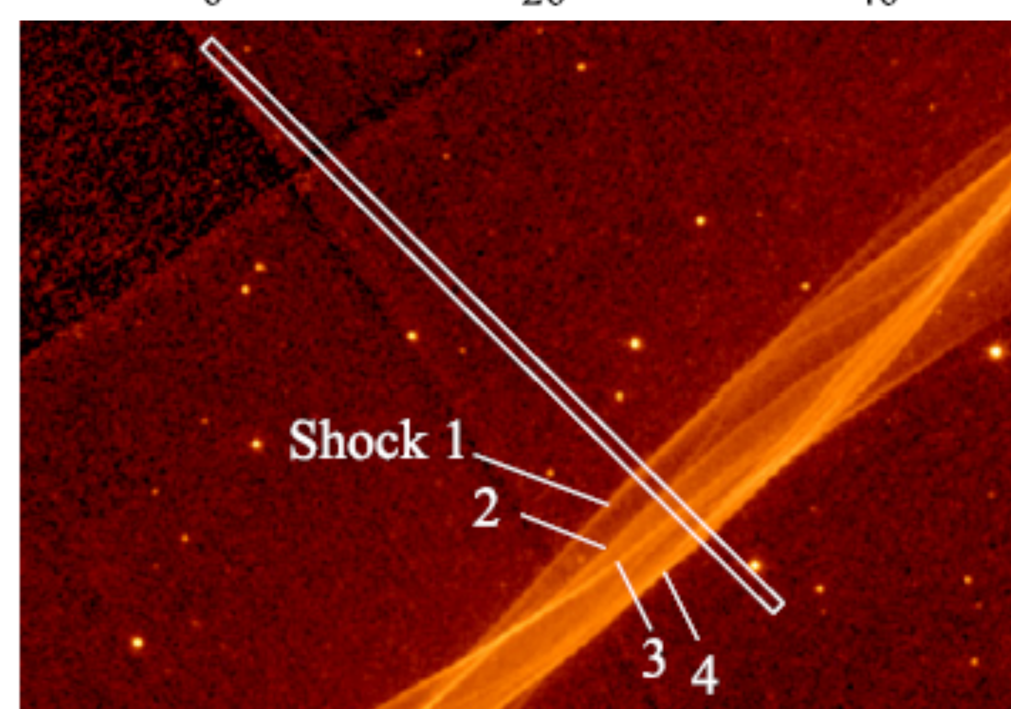

One-zone model

1. **The distribution of particles:** **"i" represents e or p**

$$N(P_i) = N_{0,i}\exp\left(-\frac{P_i}{P_{i,cut}}\right)\begin{cases} P_i^{-\alpha} & \text{if} \quad P_i < P_{\rm br} \\ P_{i,{\rm br}}P_i^{-(\alpha+1)} & \text{if} \quad P_i \geq P_{\rm br}\ , \end{cases}$$

2. **Kep=0.01, and both leptonic (Synch, Brem and IC) and hadronic (pp) emissions are considered in our fitting.**
3. **For comparison, the same background photon field is assumed for all SNRs (CMB and IR) .**
4. **Distance, Age, Shock velocity, The gas density from literature**

$$\frac{P_{\rm e,cut}}{\rm GeV/c} = 1.25 \times 10^6 \left(\frac{T_{\rm age}}{\rm Year}\right)^{-1}\left(\frac{B}{100\mu{\rm G}}\right)^{-2}$$

5-6 free parameters

MCMC method is applied to constrain these model parameters.

The Sample

SNR Name	Other Name	Radiu pc	Distance Kpc	Age kyr	n cm^{-3}	V_{shock} Km/s	The data of observations Radio	X-ray	GeV	TeV	References
G006.4−00.1	W28	~ 13	~ 2.0	40(33-150)	~ 100	60-80	✓		✓	✓	[1-4]
G008.7−00.1	W30	~ 26	~4.0	25(15-28)	~ 100	530-750	✓		✓		[5][6]
G023.3−00.3	W41	~ 19	~ 4.2	~ 100	~ 10	110	✓	T	✓	✓	[7][8]
G031.9−00.0	3C 391	~ 7	~ 7.2	~ 4	~ 300	620-730	✓		✓		[9-12]
G033.6+00.1	Kes 79	~ 9.6	~ 7.0	~ 4.4-6.7	~ 3(1-5)	400 ± 5	✓		✓		[13-15]
G034.7-00.0	W44	~ 12.5	~ 3.0	~ 20	~ 200	100-150	✓		✓		[16-18]
G043.3-00.2	W49B	~ 5	~ 10	~ 5.7(5-6)	~ 700	~ 400	✓		✓	✓	[19][20]
G049.2-00.7	W51C	~ 18	~ 4.3	~ 30	~ 10	~ 100	✓	T	✓	✓	[21-24]
G073.9+00.9		~ 16/5.2	~ 4.0/1.3	~ 11-12	~ 10	~ 200-300	✓	T	✓		[25][26]
G074.0-08.5	Cygnus loop	~ 16	~ 0.54	~ 14	~ 5.0	240-330	✓		✓		[27-30]
G089.0-04.7	HB21	~ 26	~ 1.7	~ 40(36 or 45)	~ 15	~ 125	✓		✓		[31-35]
G109.1-0.1	CTB109	~ 16	~ 3.1	~ 9.0(9.0-9.2)	~ 1.1	~ 230 ± 5	✓	T	✓		[36][37]
G120.1-01.4	Tycho	~ 3.3	~ 3.0	~ 0.44	~ 10/0.3	4600-4800	✓	✓	✓	✓	[38][39]
G132.7-00.3	HB3	~ 26.4	~ 2.2	~ 30.0	~ 2.0	303-377	✓		✓		[40-42]
G150.3+04.5		~ 9.4	~ 0.40	~ 1.5(0.5-5)	~ 1.0	?	✓		✓		[43]
G160.9-02.6	HB9	~ 15	~ 0.8	5.3(4-7)	~ 0.1	~ 740	✓	T	✓		[44][45]
G166.0+04.3		~ 26	~ 4.5	24.0	~ 0.01	~ 680	✓		✓		[46][47]
G180.0+01.7	S147	~ 38	~ 1.3	30(20-10)	~ 250(100-500)	~ 500	✓		✓		[48][49]
G189.1-03.0	IC 443	~ 11	~ 1.5	~ 30	~ 140	60-100	✓		✓	✓	[50-52]
G205.5+0.5	Monoceros	~ 63.36	~ 1.98	~ 30	~ 3.6	~ 50	✓		✓		[53-55]
G260.4-03.4	Puppis A	~ 15	~ 2.2	4.45(3.75-5.20)	~ 4.0	700-2500	✓		✓	T	[56-59]
G266.2-01.2	RX J0852-4622	~ 13	~ 0.75	2.7(1.7-4.3)	~ 3.8	~ 3000	✓	✓	✓	✓	[60][61]
G296.5+10.0		~ 26	~ 2.1	~ 10.0	~ 13.0	~ >35	✓		✓		[62][63]
G304.6-00.1	Kes 17	~ 10	~ 10	4.2(2-5.2)	~ 10	150-200	✓		✓		[64][65]
G315.4-02.3	RCW 86	~ 15	~ 2.5	~ 1.8	~ 0.1-2.0	700-2000	✓	✓	✓	✓	[66-68]
G326.3-01.8	MSH 15-56	~ 22.2	~ 4.1	~ 10.0(10-16.5)	~ 0.1/1.0	500-860	✓		✓		[67][69][70]
G327.6+14.6	SN 1006 (NE)	~ 9.0	~ 2.2	~ 1.0	~ 0.085	3200-5800	✓	✓	✓	✓	[71][72]
G332.4-00.4	RCW 103	~ 5	~ 3.3	~ 2.0	~ 10	~ 1100	✓		✓		[73-75]
G337.0-00.1	CTB 33	~ 2.55	~ 11.0	~ 5.0	~ 60	?	✓		✓		[76-78]
G347.3-00.5	RX 1713.7-3946	~ 10	~ 1.0	~ 1.6	~ 0.01	~ 5000	✓	✓	✓	✓	[82-84]
G348.5+00.1	CTB 37A	~ 10	~ 7.9	~ 30	~ 100	75-100	✓	T	✓	✓	[85-89]
G348.7+00.3	CTB 37B	~ 20	~ 13.2	~ 5	~ 10/0.5	~ 800	✓	T	✓	✓	[88-91]
G349.7+00.2		~ 3.3	~ 11.5	~ 2.8	~ 35.0	700-900	✓	T	✓	✓	[92-95]
G353.6-00.7	Hess J1731-347	~ 14.0	~ 3.2	~ 2-6	~ 0.01	~ 2100	✓	✓	✓	✓	[96][97]
G359.1-00.5	Hess J1745-303	~ 16.0	~ 4.6	~ 70	~ 100	~ 300	✓	T	✓	✓	[98-101]

Examples of spectral fits

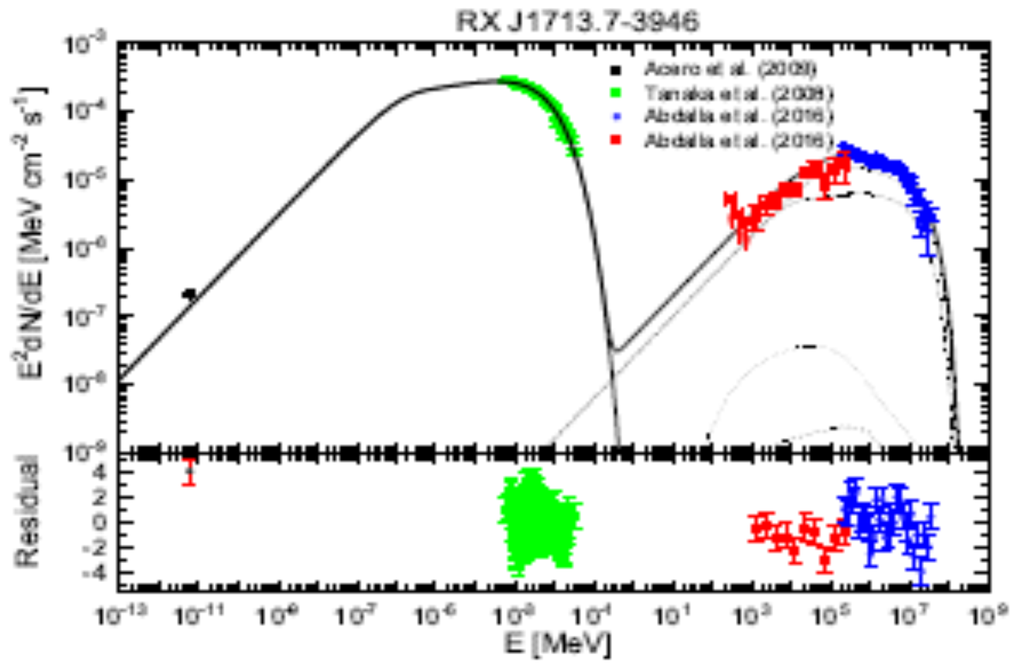

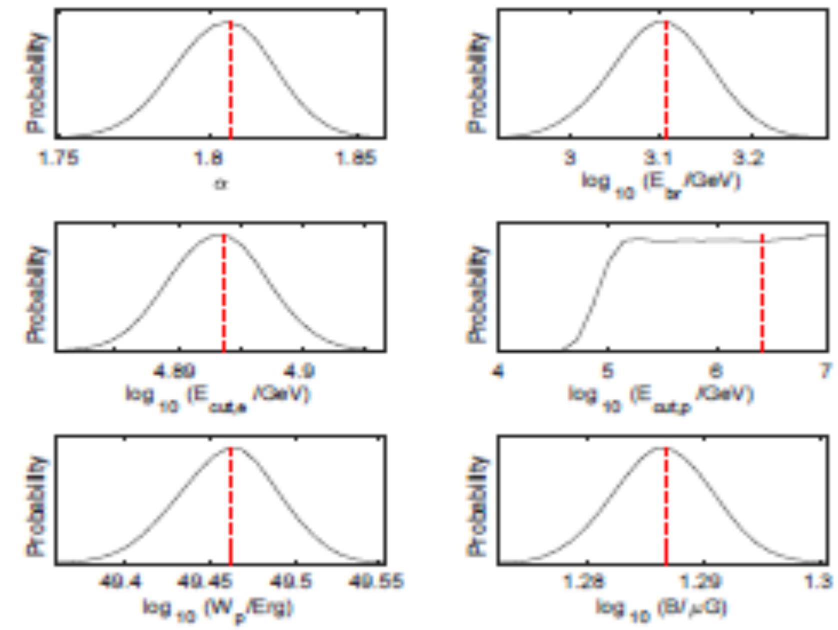

RX J1713.7-3946

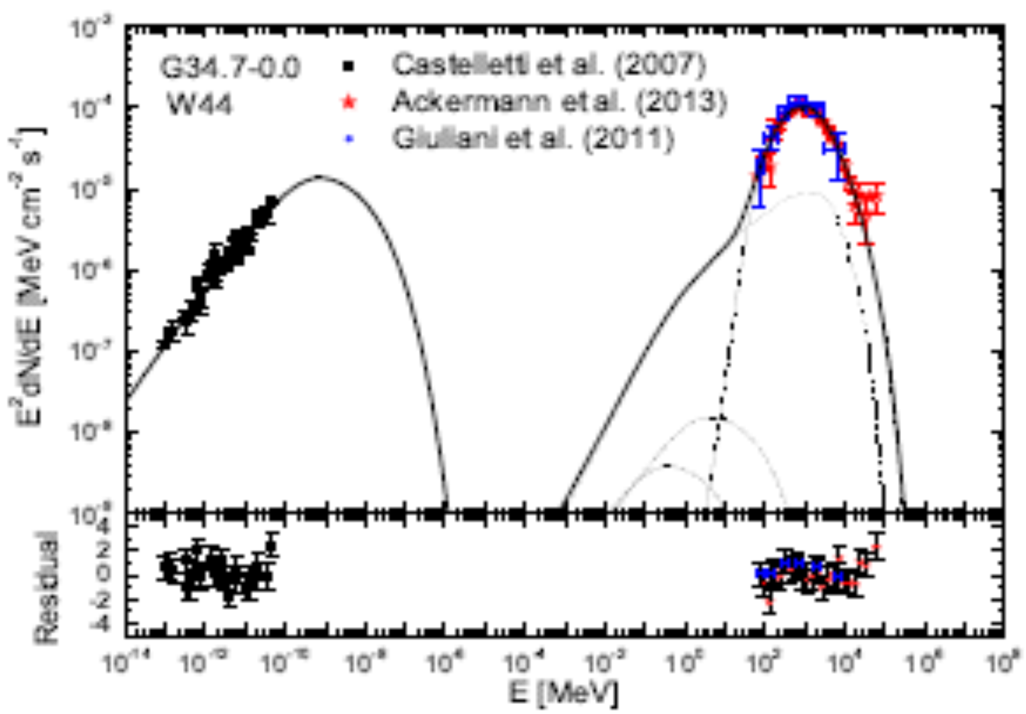

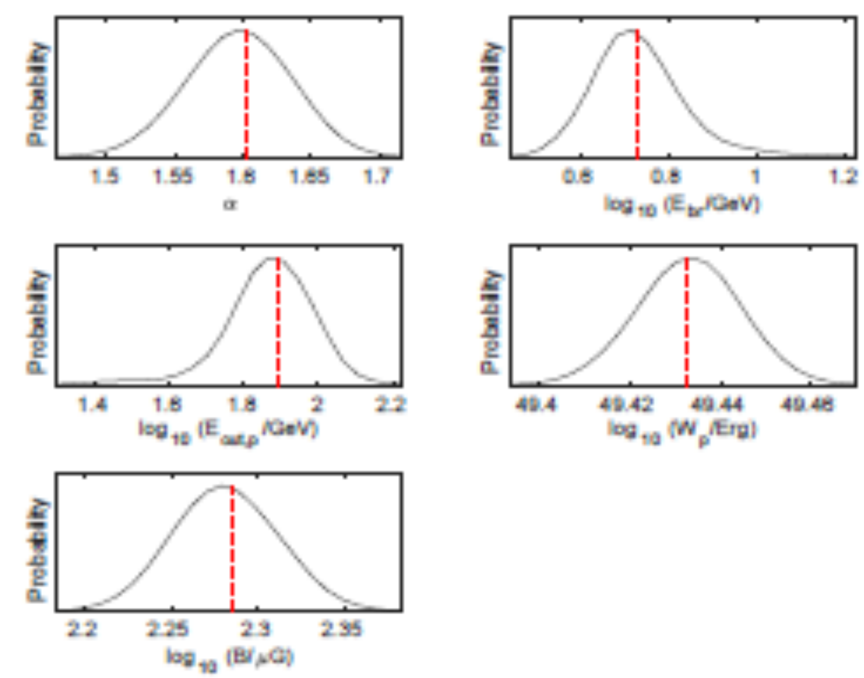

W44

Parameters

Source Name	α	$\log10 \frac{E_{br}}{GeV}$	$\log10 \frac{E_{e,cut}}{GeV}$	$\log10 \frac{E_{p,cut}}{GeV}$	$\log10 \frac{B}{\mu G}$	$\log10 \frac{W_p}{erg}$	$\frac{W_B}{W_e}$	$\frac{n}{cm^{-3}}$	$\frac{\chi^2}{NDF}$
W28	$1.76^{+0.03}_{-0.03}$	$0.18^{+0.11}_{-0.11}$	1.63	> 5.72	$1.94^{+0.04}_{-0.04}$	$49.36^{+0.02}_{-0.02}$	3.0×10^3	100	$\frac{24.3}{10} = 2.43$
W30	$1.63^{+0.10}_{-0.11}$	$0.24^{+0.33}_{-0.38}$	2.06	> 4.29	$1.86^{+0.12}_{-0.13}$	$49.69^{+0.07}_{-0.07}$	736	100	$\frac{6.0}{7} = 0.86$
W41	$1.22^{+0.04}_{-0.04}$	< -0.30	1.37	$4.52^{+0.20}_{-0.20}$	$1.87^{+0.11}_{-0.11}$	$50.21^{+0.05}_{-0.05}$	464	10	$\frac{12.6}{12} = 1.05$
3C391	$1.99^{+0.05}_{-0.05}$	$1.15^{+0.14}_{-0.14}$	1.86	> 3.81	$2.31^{+0.04}_{-0.04}$	$49.03^{+0.03}_{-0.03}$	619	300	$\frac{37.1}{19} = 1.95$
Kes79	$2.11^{+0.05}_{-0.05}$	$0.71^{+0.15}_{-0.15}$	2.89	> 4.32	$1.74^{+0.04}_{-0.04}$	$49.47^{+0.04}_{-0.04}$	28.9	100.0	$\frac{66}{23} = 2.54$
W44	$1.60^{+0.04}_{-0.04}$	$0.73^{+0.09}_{-0.09}$	1.23	$1.87^{+0.11}_{-0.09}$	$2.28^{+0.03}_{-0.03}$	$49.43^{+0.01}_{-0.01}$	1.48×10^3	200	$\frac{44.4}{48} = 0.93$
W49B	$1.47^{+0.04}_{-0.04}$	$-0.21^{+0.23}_{-0.24}$	1.55	$3.70^{+0.13}_{-0.13}$	$2.40^{+0.06}_{-0.06}$	$49.43^{+0.02}_{-0.02}$	235	700	$\frac{18.9}{20} = 1.00$
W51C	$1.56^{+0.02}_{-0.02}$	$0.31^{+0.08}_{-0.08}$	1.64	$4.39^{+0.30}_{-0.29}$	$2.08^{+0.03}_{-0.03}$	$49.83^{+0.01}_{-0.01}$	708	100	$\frac{59.7}{29} = 2.06$
W51C[b]	$1.64^{+0.02}_{-0.02}$	$0.32^{+0.05}_{-0.05}$	1.57	> 5.78	$2.02^{+0.03}_{-0.03}$	$49.79^{+0.01}_{-0.01}$	201	100	$\frac{34.9}{29} = 1.20$
G73.9+0.9[c]	$0.78^{+0.19}_{-0.19}$	$0.96^{+0.09}_{-0.09}$	$0.96^{+0.09}_{-0.09}$	$0.96^{+0.09}_{-0.09}$	$1.57^{+0.05}_{-0.05}$	$49.34^{+0.04}_{-0.04}$	393	10	$\frac{22.4}{13} = 1.72$
Cygnus Loop	$2.01^{+0.05}_{-0.05}$	$0.69^{+0.09}_{-0.09}$	2.85	> 4.09	$1.47^{+0.02}_{-0.02}$	$48.72^{+0.02}_{-0.02}$	232	5.0	$\frac{21.9}{19} = 1.15$
HB21	$1.21^{+0.10}_{-0.10}$	$0.61^{+0.08}_{-0.08}$	$0.73^{+0.07}_{-0.07}$	$0.77^{+0.07}_{-0.06}$	$1.74^{+0.02}_{-0.02}$	$49.42^{+0.01}_{-0.01}$	562	15	$\frac{36.4}{21} = 1.73$
CTB109	$1.94^{+0.09}_{-0.09}$	$2.66^{+0.38}_{-0.81}$	3.28	> 4.82	$1.47^{+0.17}_{-0.20}$	$49.84^{+0.12}_{-0.12}$	19.6	1.1	$\frac{20.9}{8} = 2.61$
Tycho	$2.15^{+0.02}_{-0.02}$	$3.37^{+0.12}_{-0.12}$	$4.14^{+0.08}_{-0.09}$	> 5.04	$2.15^{+0.04}_{-0.05}$	$49.01^{+0.08}_{-0.08}$	23.5	0.3	$\frac{55}{35} = 1.57$
Tycho	$2.16^{+0.02}_{-0.02}$	$3.36^{+0.11}_{-0.11}$	$4.06^{+0.07}_{-0.07}$	> 4.93	$2.29^{+0.04}_{-0.05}$	$48.78^{+0.07}_{-0.07}$	92.2	10.0	$\frac{44}{35} = 1.26$
HB3	$2.07^{+0.10}_{-0.10}$	$0.76^{+0.14}_{-0.14}$	3.50	> 4.57	$1.07^{+0.03}_{-0.03}$	$50.03^{+0.03}_{-0.03}$	7.49	2.0	$\frac{16.8}{18} = 0.93$
G150.3+4.5	$1.73^{+0.22}_{-0.22}$	$2.65^{+0.36}_{-0.42}$	6.04	> 6.37	$0.45^{+0.13}_{-0.13}$	$48.33^{+0.05}_{-0.05}$	1.42	1.0	$\frac{11.5}{12} = 0.96$
HB9	$2.23^{+0.06}_{-0.06}$	$0.89^{+0.12}_{-0.12}$	5.07	> 5.68	$0.67^{+0.04}_{-0.04}$	$50.10^{+0.05}_{-0.05}$	0.16	0.1	$\frac{15.2}{14} = 1.09$
G166.0+4.3[c]	$1.32^{+0.17}_{-0.18}$	1.87	1.87	$1.87^{+0.14}_{-0.15}$	$0.57^{+0.24}_{-0.24}$	$50.92^{+0.26}_{-0.25}$	0.12	0.01	$\frac{6.92}{5} = 1.38$
G166.0+4.3[c]	$1.26^{+0.17}_{-0.18}$	1.18	1.18	$1.18^{+0.16}_{-0.16}$	$1.62^{+0.10}_{-0.10}$	$49.18^{+0.07}_{-0.07}$	717	10.0	$\frac{7.70}{5} = 1.54$
S147	$1.36^{+0.06}_{-0.06}$	$-0.14^{+0.12}_{-0.13}$	0.09	> 3.86	$2.77^{+0.09}_{-0.09}$	$47.71^{+0.05}_{-0.05}$	2.7×10^8	250	$\frac{17.3}{17} = 1.02$
S147	$1.53^{+0.11}_{-0.11}$	$0.51^{+0.12}_{-0.12}$	3.57	> 4.65	$1.03^{+0.05}_{-0.05}$	$49.94^{+0.04}_{-0.04}$	31.6	1.0	$\frac{19.8}{17} = 1.16$
IC 443	$1.38^{+0.03}_{-0.03}$	$0.12^{+0.07}_{-0.07}$	1.35	$3.22^{+0.10}_{-0.10}$	$2.14^{+0.02}_{-0.02}$	$48.96^{+0.01}_{-0.01}$	2.28×10^3	140	$\frac{92.0}{64} = 1.44$
Monoceros Loop	$1.63^{+0.02}_{-0.02}$	$0.74^{+0.11}_{-0.11}$	2.97	> 5.77	$1.31^{+0.03}_{-0.03}$	$50.29^{+0.03}_{-0.03}$	224	3.6	$\frac{42.5}{16} = 1.63$
Puppis A	$2.08^{+0.02}_{-0.02}$	$3.23^{+0.48}_{-0.56}$	2.50	> 4.57	$1.97^{+0.02}_{-0.02}$	$49.53^{+0.04}_{-0.04}$	500	4.0	$\frac{48.8}{30} = 1.46$
RX J0852-4622[d]	$2.21^{+0.04}_{-0.04}$		$4.30^{+0.06}_{-0.06}$	> 5.15	$1.03^{+0.04}_{-0.04}$	$49.61^{+0.05}_{-0.05}$	2.79	0.01	$\frac{27.8}{16} = 1.74$
RX J0852-4622	$1.93^{+0.05}_{-0.05}$	$1.13^{+0.18}_{-0.16}$	$4.38^{+0.06}_{-0.06}$	> 5.15	$1.04^{+0.04}_{-0.04}$	$49.70^{+0.04}_{-0.04}$	2.6	0.01	$\frac{18.6}{15} = 1.24$
G296.5+10.0	$1.86^{+0.08}_{-0.08}$	> 3.75	0.59	> 3.99	$2.73^{+0.13}_{-0.13}$	$48.55^{+0.14}_{-0.14}$	1.15×10^7	13.0	$\frac{4.3}{5} = 0.86$
Kes 17	$2.01^{+0.18}_{-0.17}$	> 3.52	3.03	> 4.20	$1.79^{+0.17}_{-0.17}$	$50.33^{+0.11}_{-0.11}$	7.0	10.0	$\frac{1.06}{2} = 0.53$
RCW 86	$2.26^{+0.02}_{-0.02}$	$3.92^{+0.08}_{-0.09}$	$4.42^{+0.04}_{-0.03}$	> 5.23	$1.44^{+0.02}_{-0.02}$	$49.82^{+0.03}_{-0.03}$	15.3	0.01	$\frac{31.5}{22} = 1.43$
MSH 15-56	$1.43^{+0.14}_{-0.14}$	$2.13^{+0.17}_{-0.20}$	2.40	> 3.06	$1.81^{+0.09}_{-0.08}$	$51.05^{+0.13}_{-0.13}$	34.3	0.1	$\frac{10.1}{7} = 1.44$
MSH 15-56	$1.61^{+0.12}_{-0.12}$	$1.17^{+0.08}_{-0.11}$	3.02	> 3.83	$1.60^{+0.10}_{-0.10}$	$50.75^{+0.06}_{-0.06}$	9.7	1.0	$\frac{8.0}{7} = 1.14$
SN 1006	$2.09^{+0.04}_{-0.04}$	> 4.84	$3.86^{+0.10}_{-0.10}$	> 4.92	$1.77^{+0.05}_{-0.06}$	$48.72^{+0.07}_{-0.07}$	240	0.085	$\frac{49.0}{35} = 1.40$
RCW 103	$2.11^{+0.08}_{-0.08}$	> 3.86	3.90	> 4.87	$1.45^{+0.08}_{-0.08}$	$50.00^{+0.06}_{-0.06}$	0.44	10	$\frac{1.0}{6} = 0.17$
CTB 33	$2.00^{+0.38}_{-0.33}$	$1.41^{+0.56}_{-0.55}$	4.67	> 5.43	$0.87^{+0.08}_{-0.08}$	$50.47^{+0.07}_{-0.07}$	0.001	60	$\frac{9.06}{5} = 1.81$
RX J1713.7-3946[a]	$1.81^{+0.02}_{-0.02}$	$3.10^{+0.05}_{-0.05}$	$4.89^{+0.004}_{-0.004}$	> 5.57	$1.29^{+0.004}_{-0.004}$	$49.46^{+0.03}_{-0.03}$	6.0	0.01	$\frac{445}{240} = 1.85$
CTB 37A	$1.47^{+0.02}_{-0.02}$	$0.36^{+0.19}_{-0.17}$	1.0	> 5.96	$2.40^{+0.12}_{-0.10}$	$49.82^{+0.02}_{-0.02}$	607	100	$\frac{23.4}{16} = 1.46$
CTB 37B	$1.49^{+0.11}_{-0.11}$	$2.40^{+0.33}_{-0.34}$	0.81	> 5.34	$2.84^{+0.15}_{-0.15}$	$50.51^{+0.04}_{-0.04}$	1.04×10^5	10	$\frac{15.6}{14} = 1.11$
CTB 37B	$1.58^{+0.07}_{-0.07}$	$3.06^{+0.19}_{-0.20}$	2.47	> 5.32	$1.97^{+0.06}_{-0.06}$	$51.60^{+0.04}_{-0.04}$	28.3	0.5	$\frac{14.1}{14} = 1.00$
G349.7+0.2	$2.06^{+0.13}_{-0.12}$	$2.82^{+0.30}_{-0.38}$	2.70	> 5.00	$2.00^{+0.12}_{-0.12}$	$50.09^{+0.04}_{-0.04}$	1.30	35	$\frac{5.2}{10} = 0.52$
Hess J1731-347	$1.86^{+0.04}_{-0.04}$	$3.65^{+0.10}_{-0.10}$	$4.27^{+0.02}_{-0.02}$	> 5.19	$1.46^{+0.02}_{-0.02}$	$49.42^{+0.04}_{-0.04}$	45.1	0.01	$\frac{283.9}{322} = 0.88$
Hess J1745-303	$1.64^{+0.04}_{-0.04}$	$0.52^{+0.20}_{-0.18}$	2.03	> 5.37	$1.66^{+0.08}_{-0.08}$	$49.53^{+0.08}_{-0.08}$	167	100	$\frac{3.62}{8} = 0.45$

Results

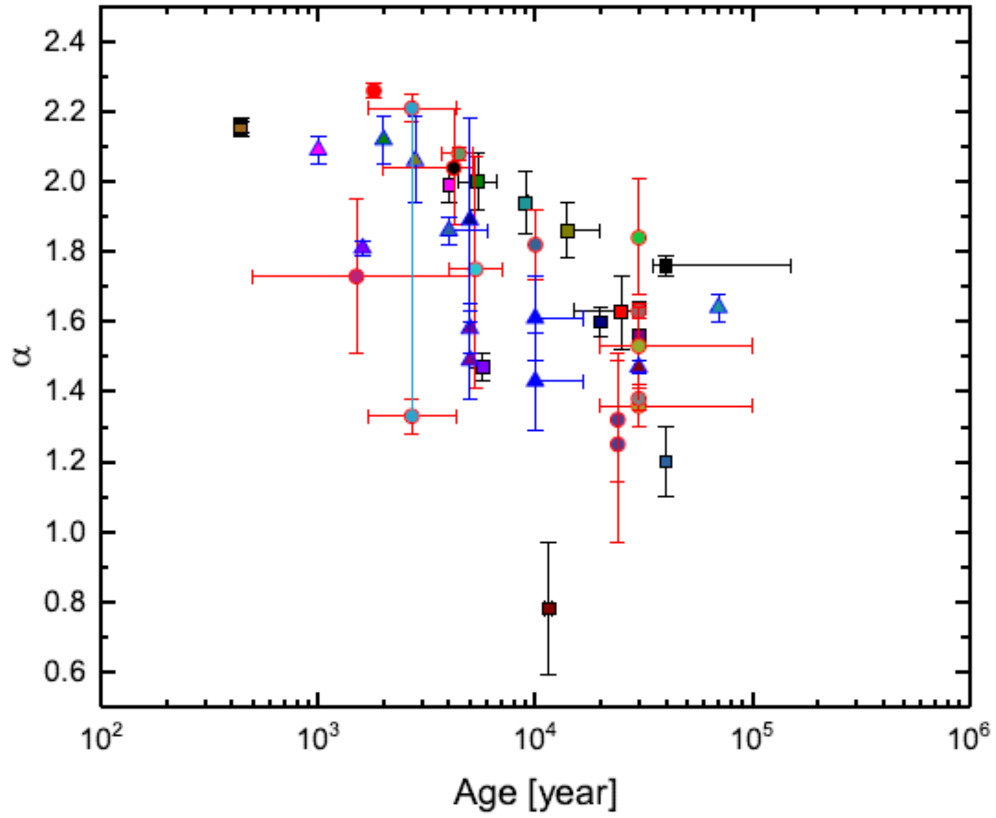

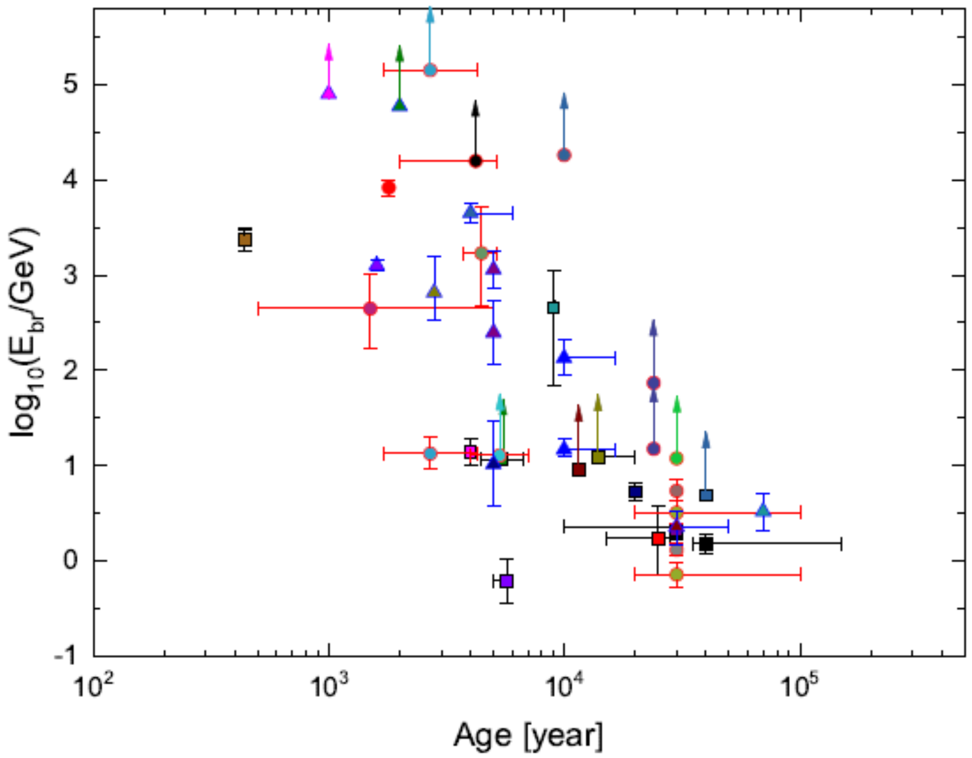

Figure (a) show there is an inverse correlation between the low-energy spectra index and age, and the spectral become harder with aging of SNRs. This result agrees with the observational fact that the radio spectrum harden with aging of SNRs (e.g. Dubner & Giacani (2015))..

Figure (b): The break energy of particle distribution decreases with the age of SNRs, which may be related to the gradual weakening of shock waves with aging in SNRs and agree with the particle acceleration model with proposed by Ohira et al. (see also Zhang et al.2017)

Results

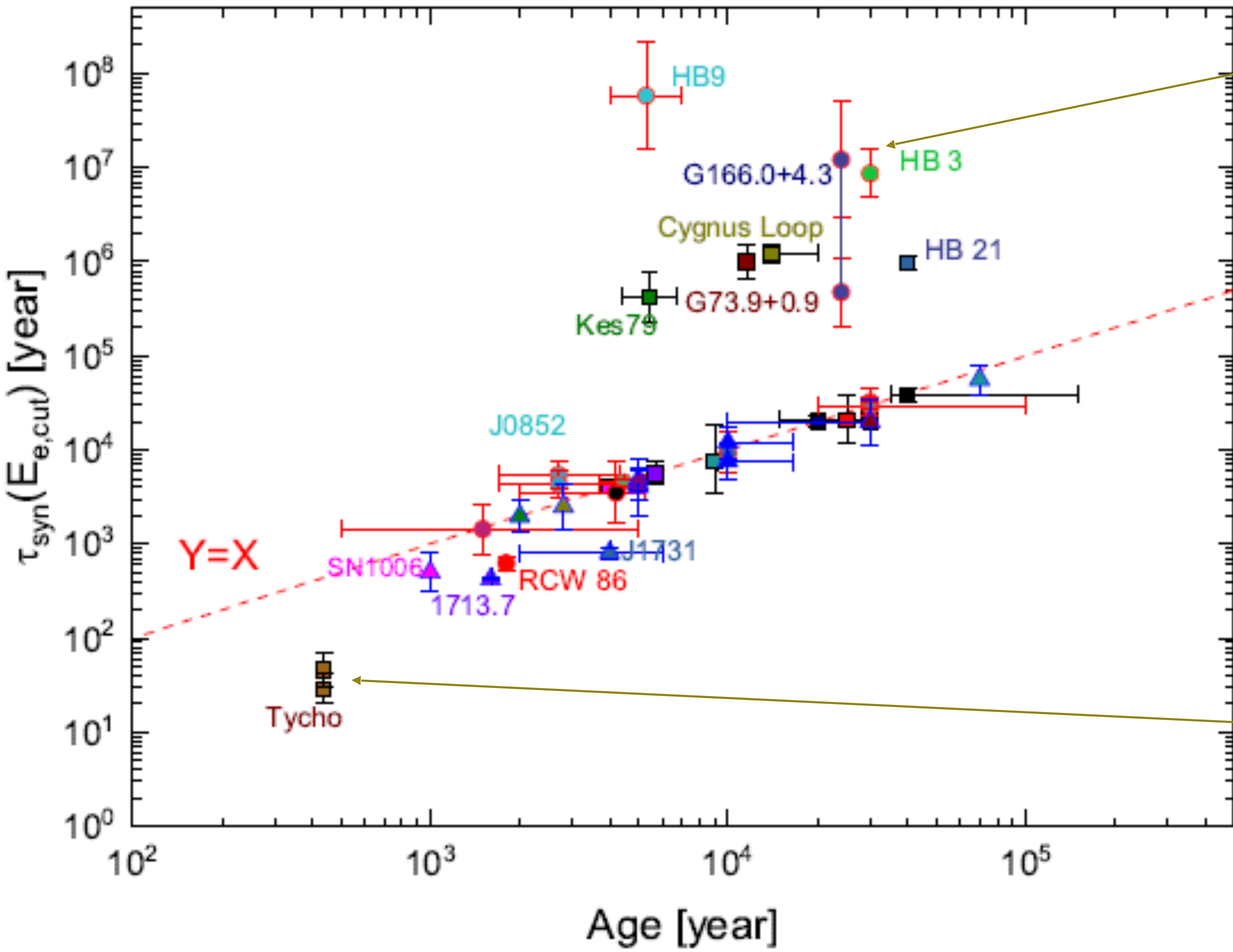

Energy loss timescale > Age may suggest escape of highest energy particles from SNRs.

Energy loss timescale < Age implying continuous particle acceleration at the cutoff energy of SNRs

For most middle-age SNRs, the energy loss timescale of electrons at the high-energy cutoff is approximately equal to the age of SNRs, implying quenching of high-energy electron acceleration (Ohira et al).

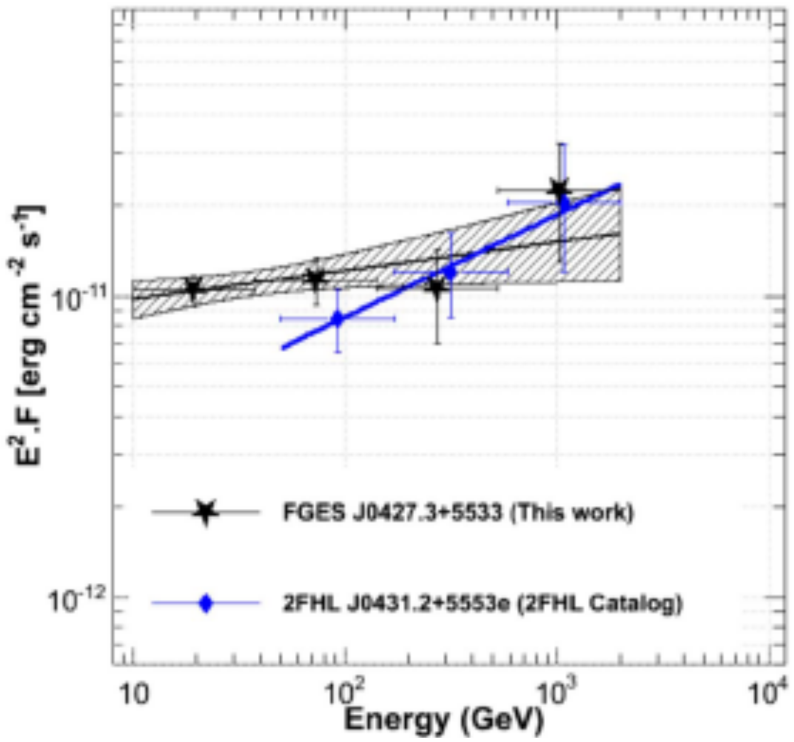

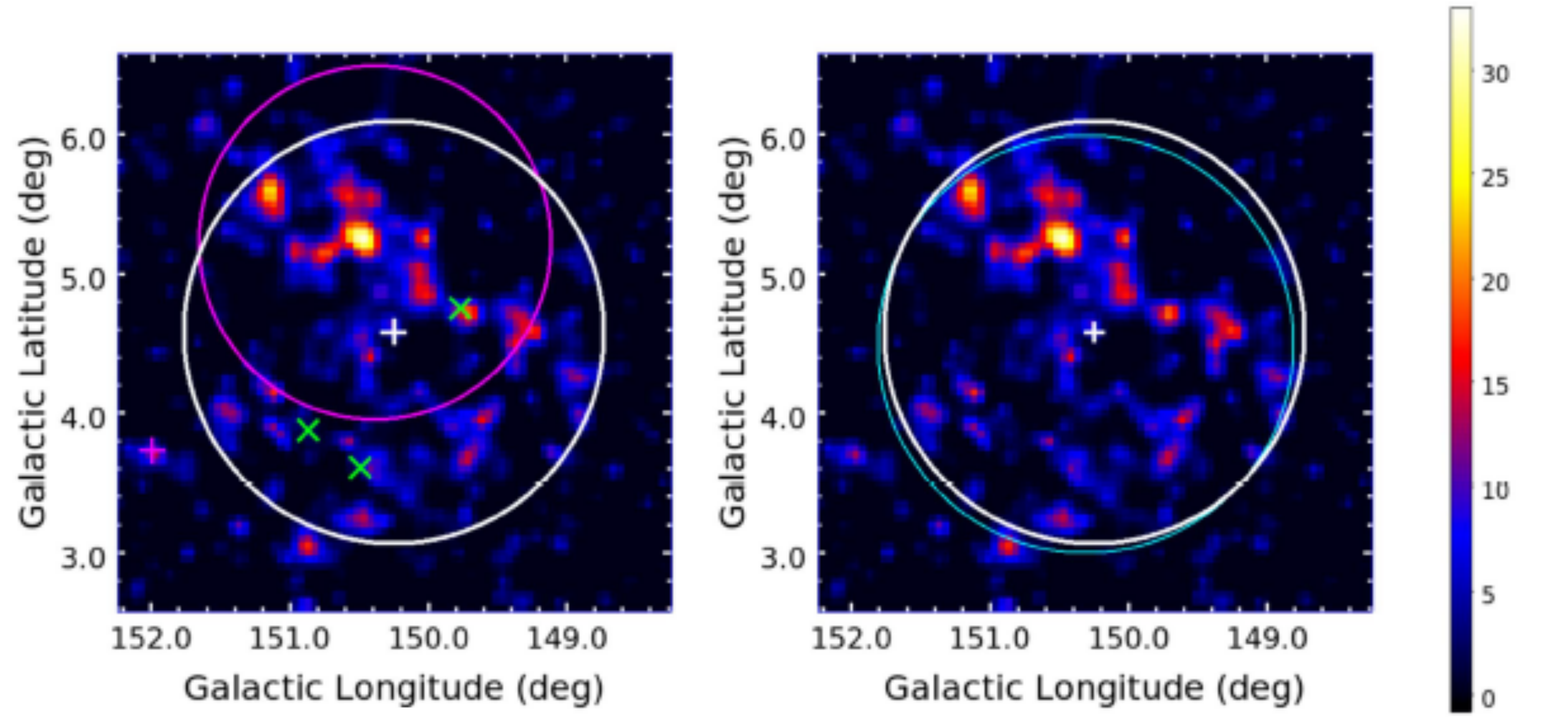

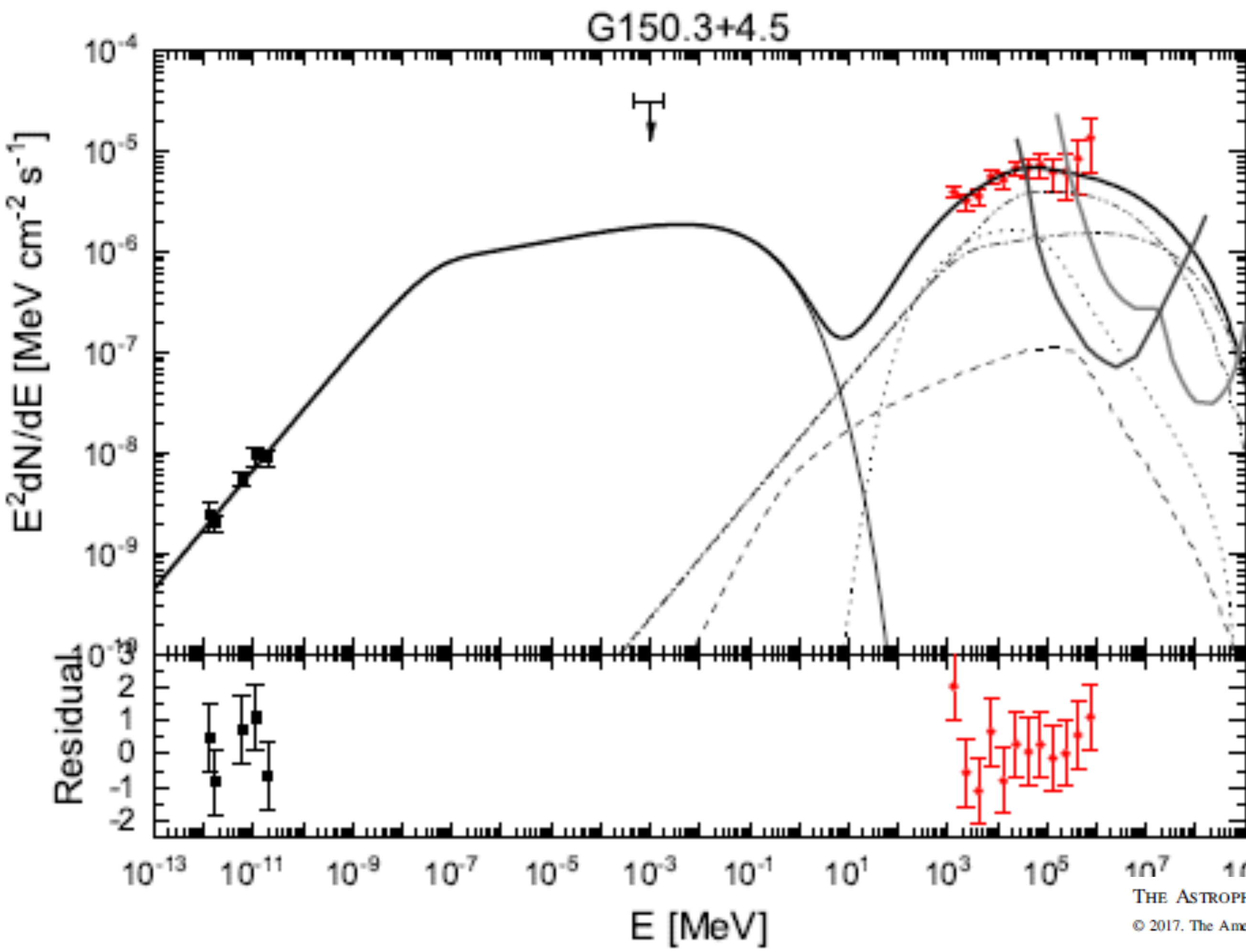

G150.3+4.5

A good LHAASO target?

The Astrophysical Journal, 843:139 (24pp), 2017 July 10
https://doi.org/10.3847/1538-4357/aa775a

Search for Extended Sources in the Galactic Plane Using Six Years of *Fermi*-Large Area Telescope Pass 8 Data above 10 GeV

M. Ackermann[1], M. Ajello[2], L. Baldini[3], J. Ballet[4], G. Barbiellini[5,6], D. Bastieri[7,8], R. Bellazzini[9], E. Bissaldi[10], E. D. Bloom[11],

Gamma-ray emission from middle-aged supernova remnants interacting with molecular clouds: the challenge for current models

Xiaping Tang,[1,2]★
[1]Max Planck Institute for Astrophysics, Karl-Schwarzschild-Str. 1, D-85741 Garching, Germany
[2] The Racah Institute of physics, The Hebrew University of Jerusalem, Jerusalem 91904, Israel

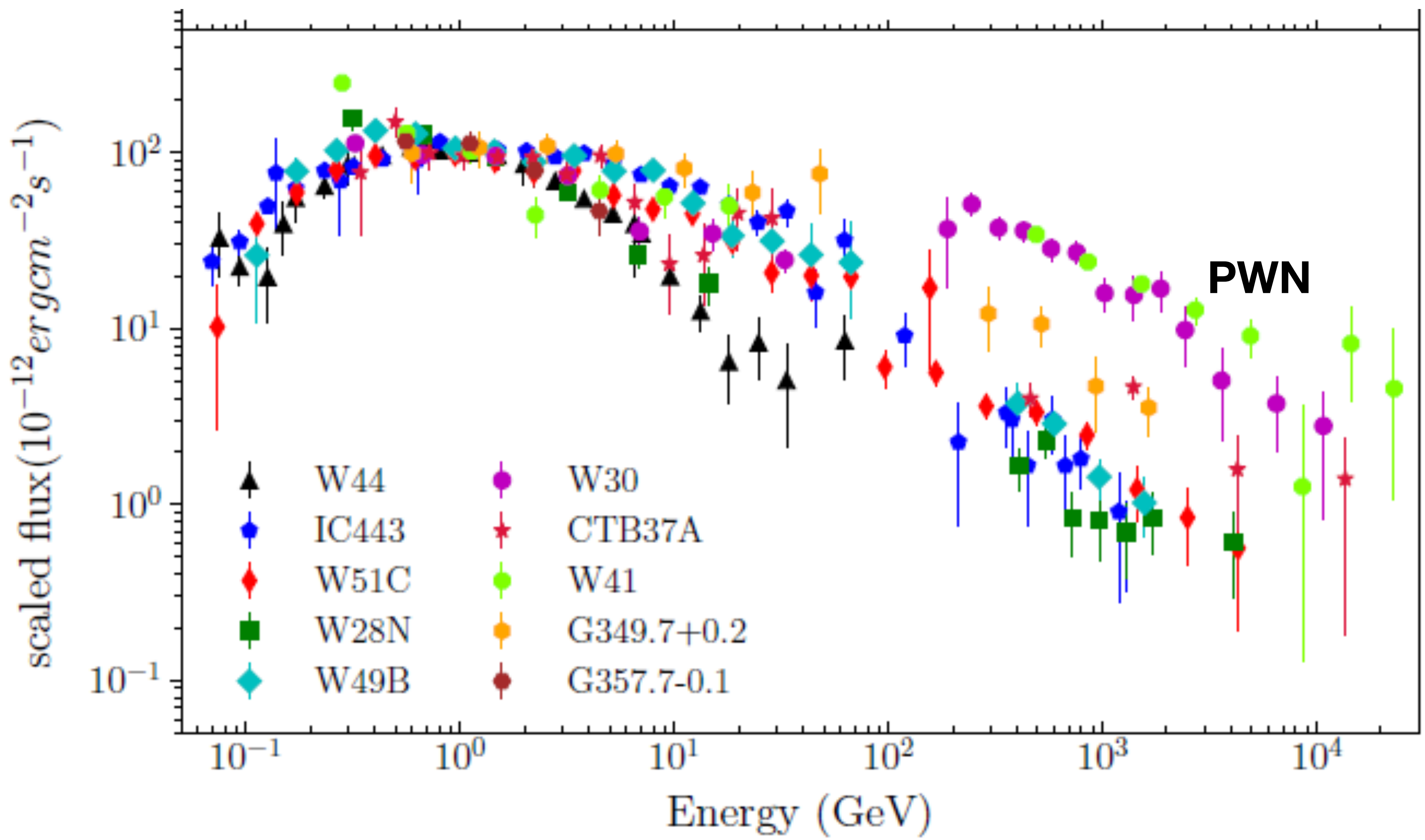

Gamma ray index does not change significantly: Implying energy-independent escape

Journal of Cosmology and Astroparticle Physics
An IOP and SISSA journal

Understanding hadronic gamma-ray emission from supernova remnants

Caprioli Damiano

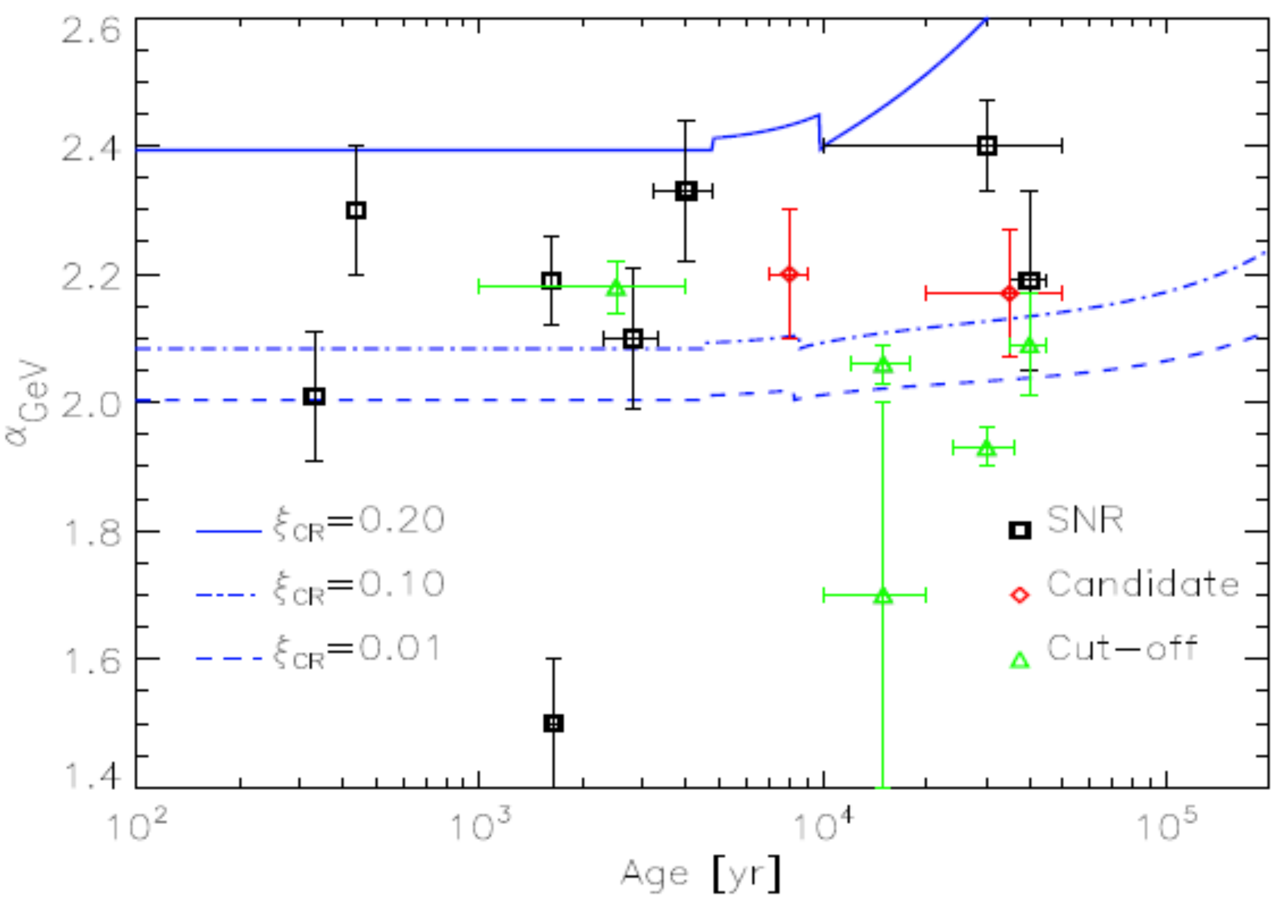

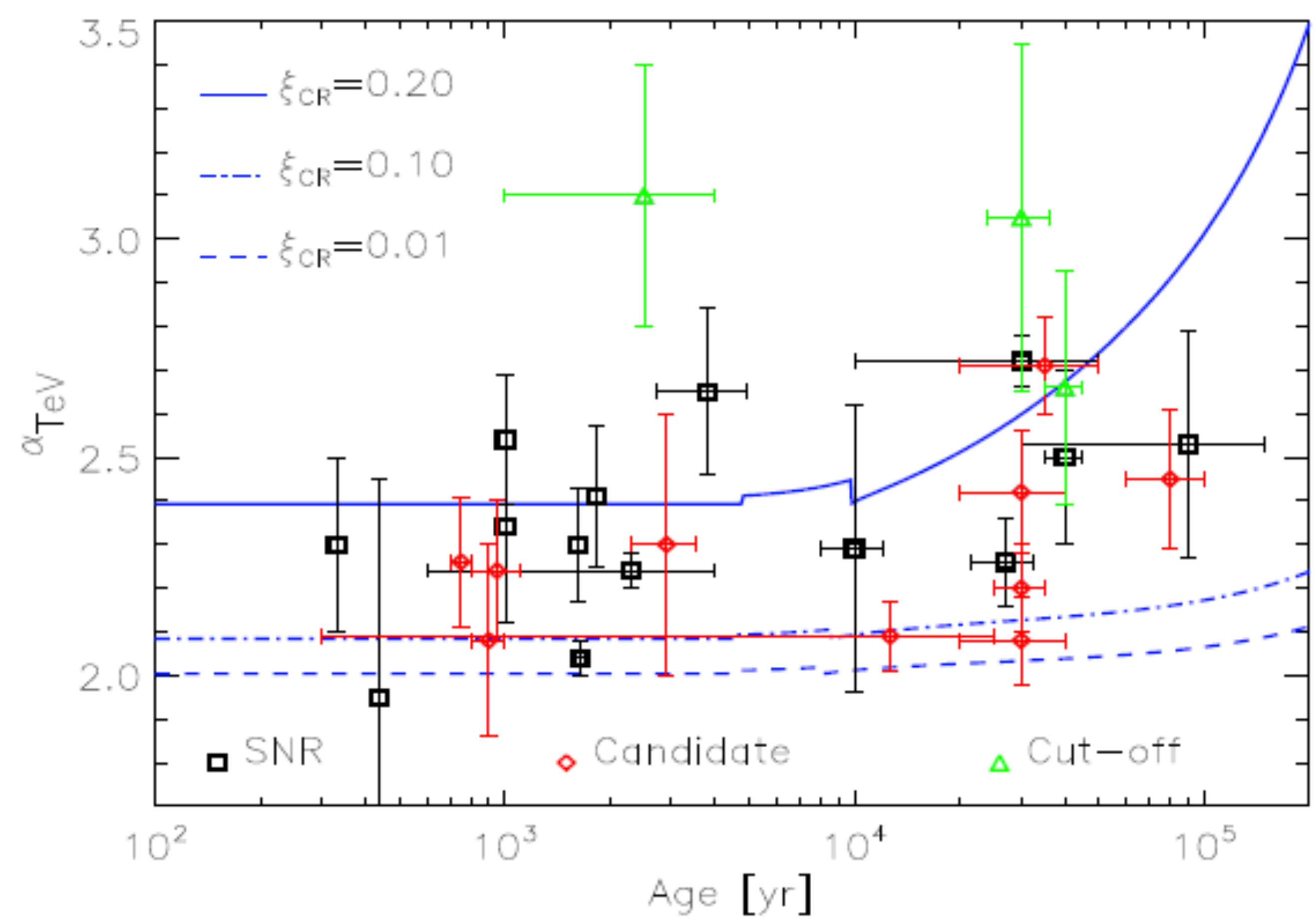

Cosmic ray injection

Energy loss timescale > Age may suggest escape of highest energy particles from SNRs.

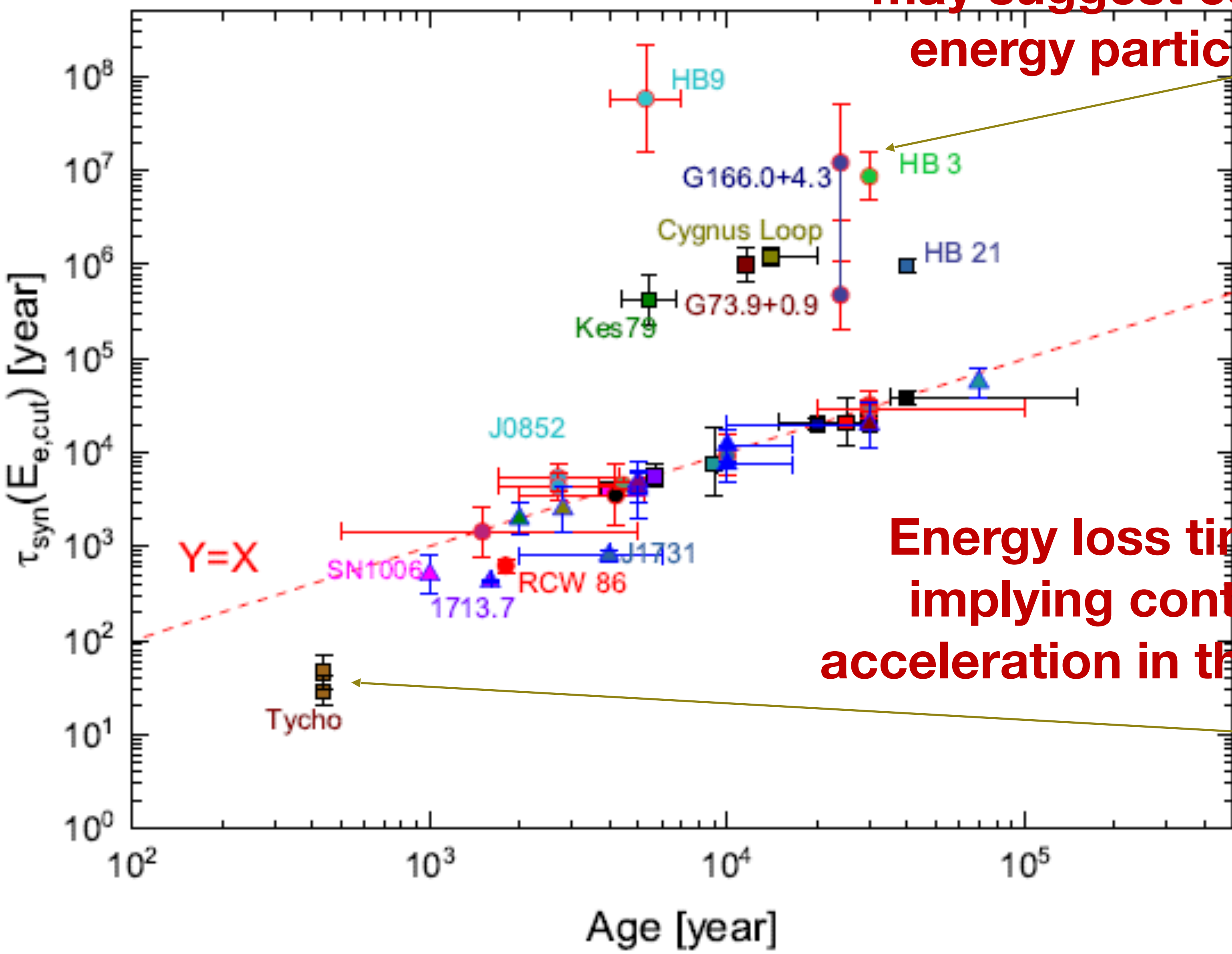

Energy loss timescale < Age implying continuous particle acceleration in the interior of SNRs

For most middle-age SNRs, the energy loss timescale of electrons at the high-energy cutoff is approximately equal to the age of SNRs, implying quenching of high-energy electron acceleration (Ohira et al).

Cosmic ray electron & positron

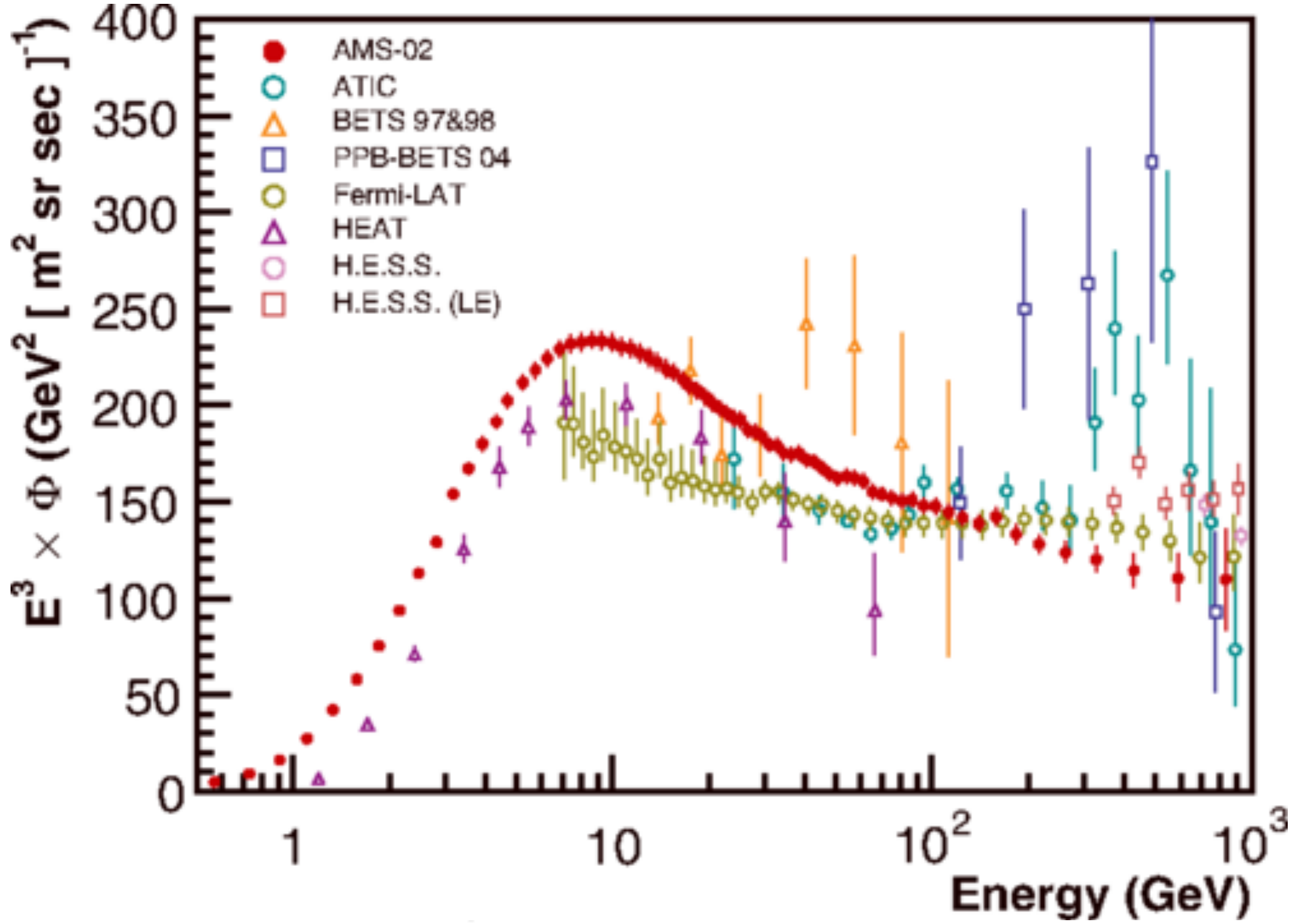

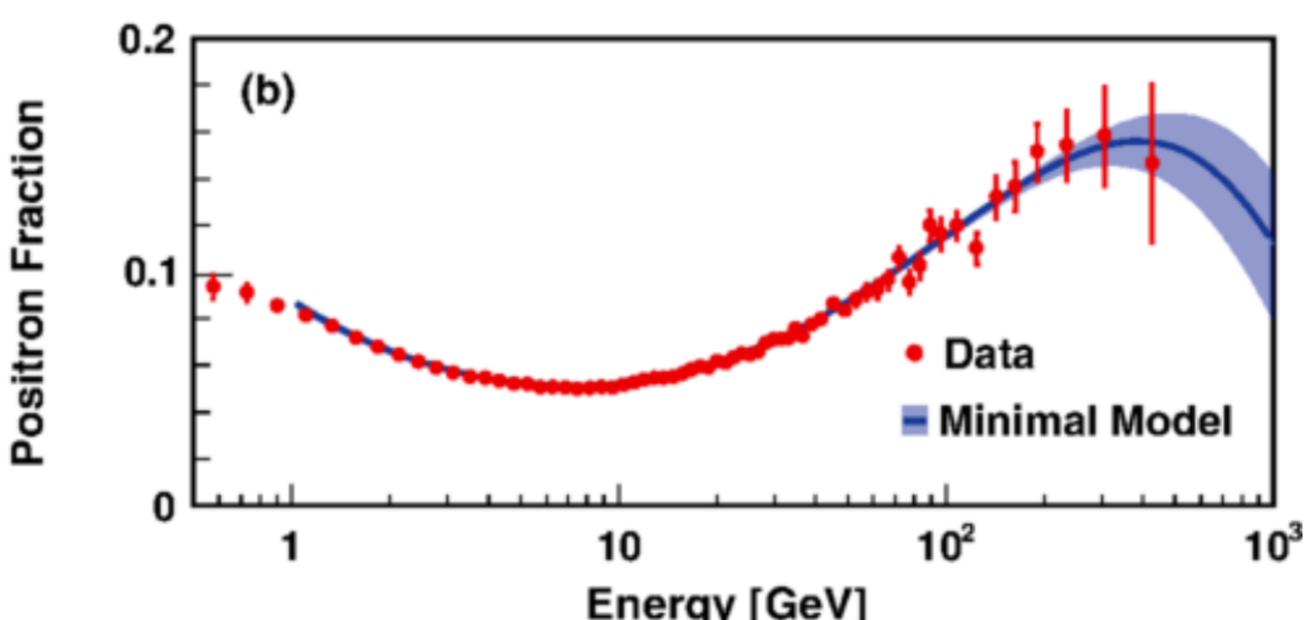

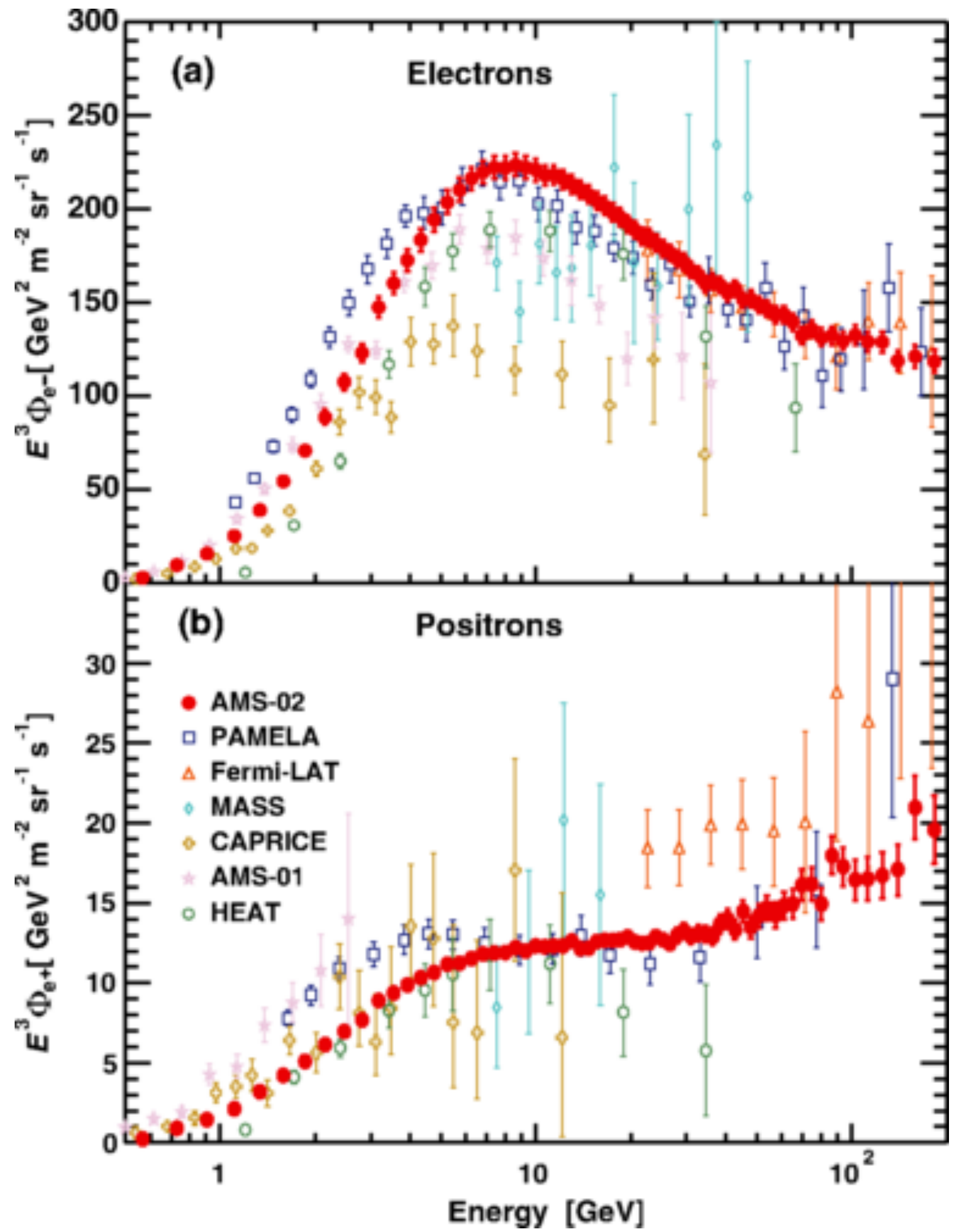

Cosmic ray electron & positron

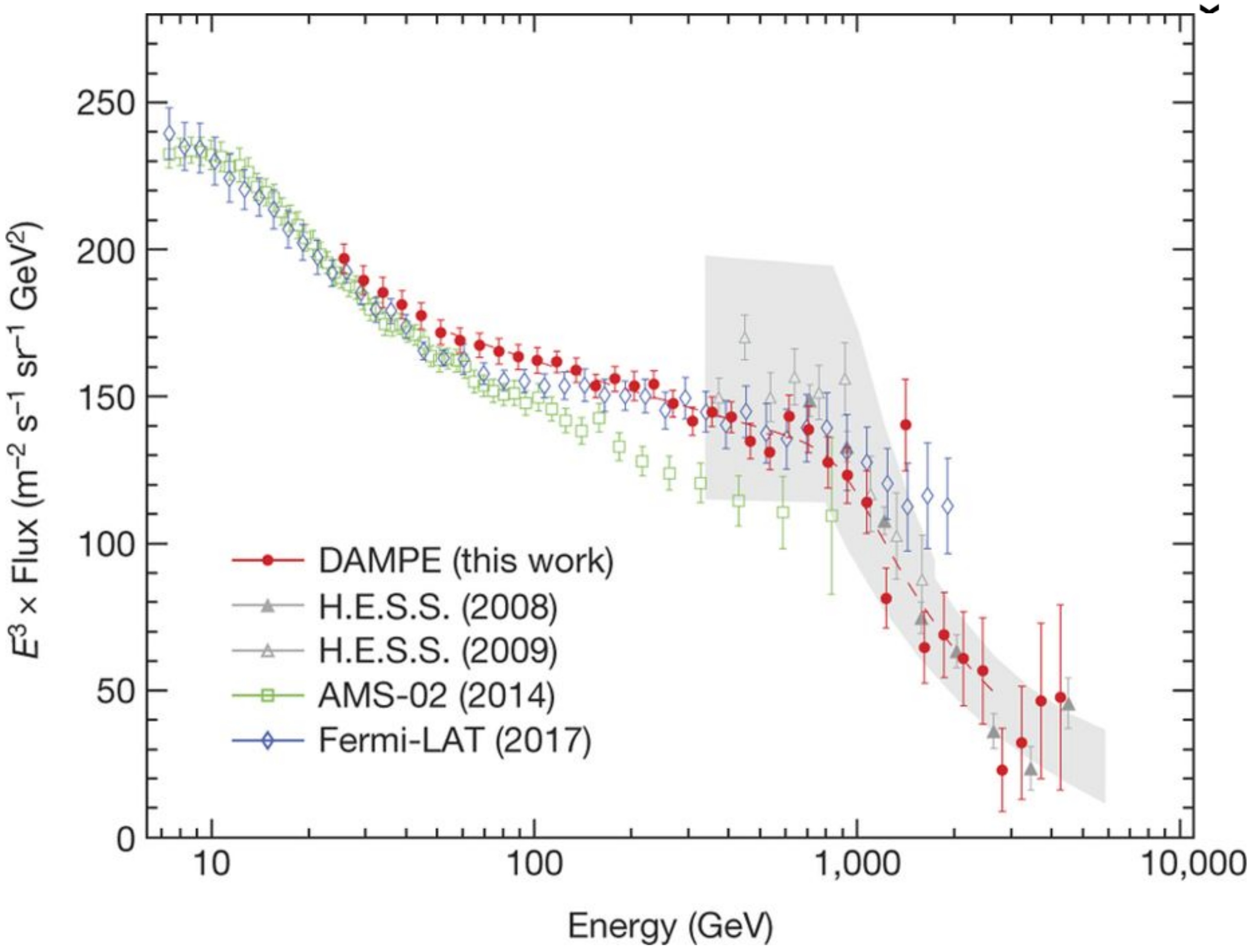

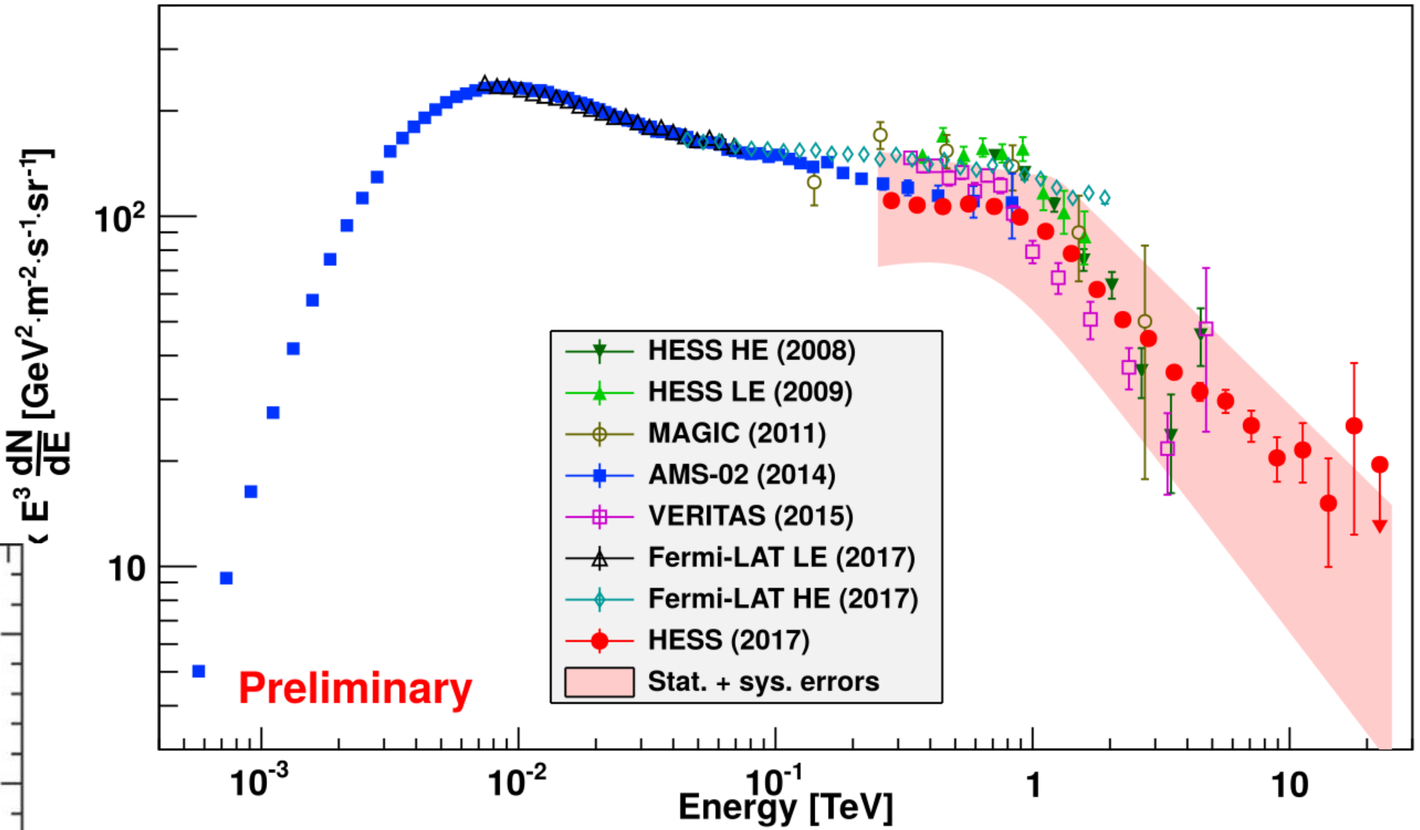

Modeling electron & positron spectra

- **Propagated Fluxes of Electrons & Positrons**

$$J_{e^-} = CE^{-\gamma}e^{-\frac{E}{E_{cut}}} + 0.6C_{e^+}E^{-\gamma_{e^+}} + C_{e^-}\begin{cases} E^{-\gamma_{e^-}^1} & E \le E_{br1} \\ E_{br1}^{\gamma_{e^-}^2-\gamma_{e^-}^1}E^{-\gamma_{e^-}^2} & E_{br1} < E \le E_{br2} \\ E_{br1}^{\gamma_{e^-}^2-\gamma_{e^-}^1}E_{br2}^{\gamma_{e^-}^3-\gamma_{e^-}^2}E^{-\gamma_{e^-}^3} & E > E_{br2} \end{cases}$$

$$J_{e^+} = CE^{-\gamma}e^{-\frac{E}{E_{cut}}} + C_{e^+}E^{-\gamma_{e^+}}$$

- **Solar Modulation**

$$J(E) = \left(\frac{E}{E+e\phi}\right)^2 J_0(E+e\phi)$$

Modeling CR Electron & Positron Spectra

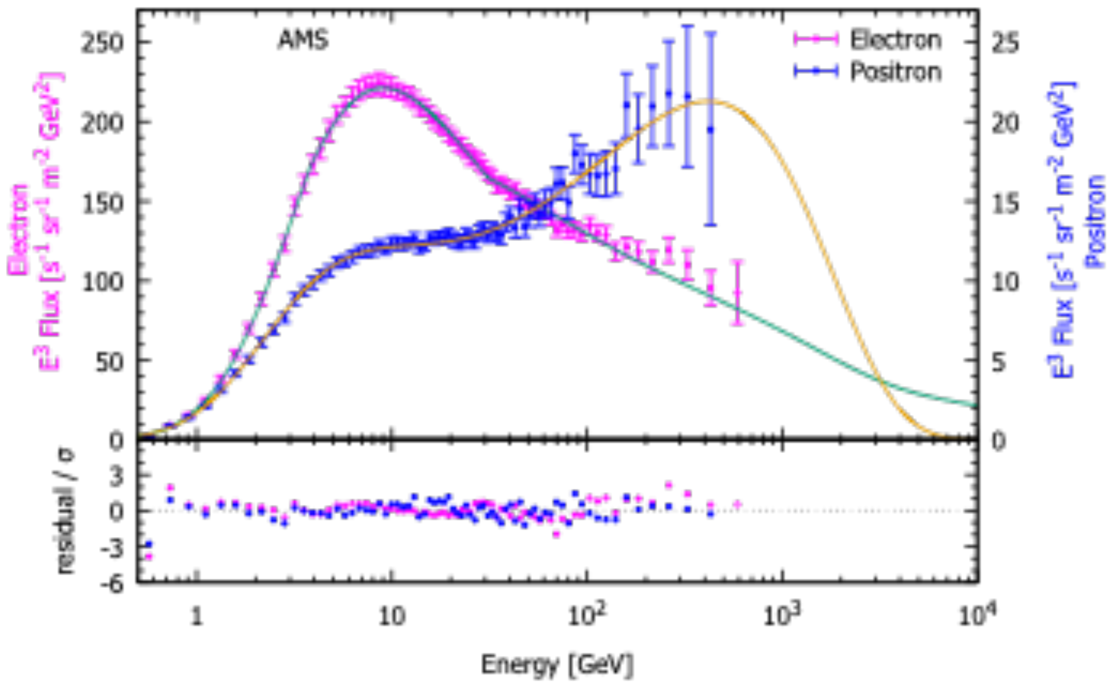

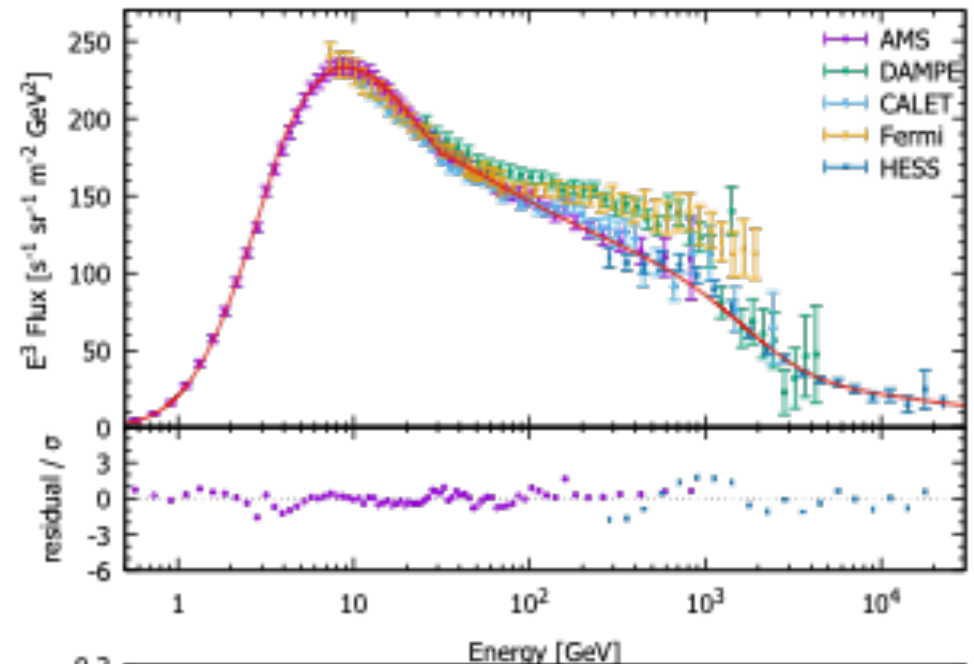

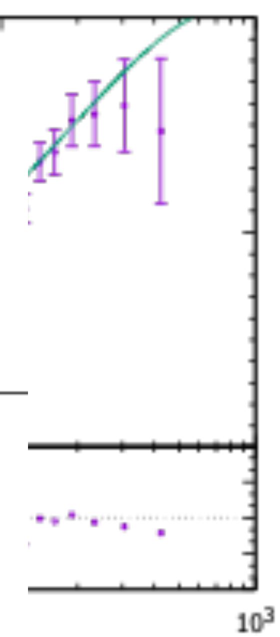

solar modulation $\phi = 1.140\,\mathrm{GV}$

$C_{e^-}{}^\dagger$	γ^1_{e-}	E_{br1}	γ^2_{e-}	E_{br2}	γ^3_{e-}	$C_{e+}{}^\dagger$	γ_{e+}	$C^\dagger$	γ	E_{cut}
1063	3.347	4.960	3.643	32.355	3.370	163.25	4.048	3.139	2.620	1100

$C^{inj\,\ddagger}_{e-}$	$\gamma^{1,inj}_{e-}$	E^{inj}_{br}	$\gamma^{2,inj}_{e-}$	$C^{inj\,\ddagger}_{e+}$	γ^{inj}_{e+}	$C^{inj\,\ddagger}$	γ^{inj}	E^{inj}_{cut}
6.612×10^{41}	3.059	40.917	2.644	1.053×10^{41}	3.683	1.050×10^{39}	2.040	1555

† with units of $\mathrm{s}^{-1}\,\mathrm{sr}^{-1}\,\mathrm{m}^{-2}\,\mathrm{GeV}^{-1}$.

‡ with units of $\mathrm{kyr}^{-1}\,\mathrm{pc}^{-3}\,\mathrm{GeV}^{-1}$.

1D Propagation Model

- **1D Steady-state Transport Equation**

$$D(E)\frac{\partial^2 N(z,E)}{\partial z^2} + \frac{\partial b(E)N(z,E)}{\partial E} + Q(z,E) = 0$$

$$D(E) = D_0\,(E/1\,\mathrm{GeV})^{\delta}, \quad b(E) = -\,\mathrm{d}E/\mathrm{d}t = b_0E^2$$

$$N(\pm H, E) = 0, \quad Q(z,E) = q(E)\theta(h - |z|)$$

$$N(z,E) = \frac{2}{b_0E^2}\sum_{m=0}^{\infty}\frac{\sin\left[\left(m+\frac{1}{2}\right)\pi\frac{h}{H}\right]}{\left(m+\frac{1}{2}\right)\pi}\cos\left[\left(m+\frac{1}{2}\right)\pi\frac{z}{H}\right]\int_E^{\infty}\mathrm{d}E' q\left(E'\right)\exp\left\{\left[\left(m+\frac{1}{2}\right)\pi\frac{\ell(E)}{H}\right]^2\left[\left(\frac{E}{E'}\right)^{1-\delta}-1\right]\right\}. \quad (4)$$

$$\ell(E) \equiv \sqrt{\frac{D_0E^{\delta-1}}{(1-\delta)b_0}}, \quad \ell\left(E_H\right) = H, \quad \ell\left(E_h\right) = h$$

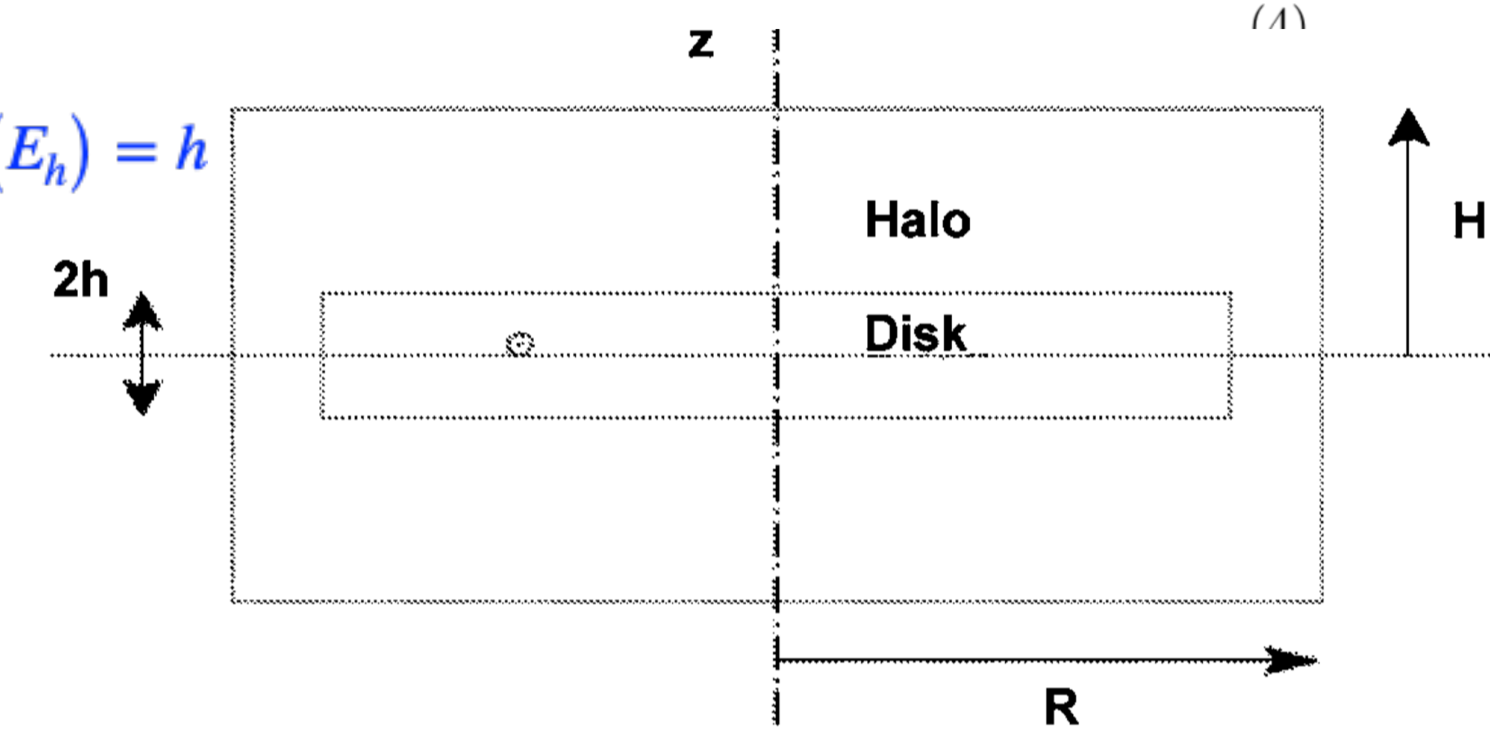

Credit: Ptuskin (2001)

1D Propagation Model

al index (z = 0) for a power-law injection

$$\gamma_a = \begin{cases} \gamma + \delta, & E < E_H \\ \gamma + \frac{\delta + 1}{2}, & E_H < E < E_h \\ \gamma + 1, & E > E_h \end{cases}$$

$$\ell(E) \equiv \sqrt{\frac{D_0 E^{\delta-1}}{(1-\delta) b_0}}, \quad \ell(E_H) = H, \quad \ell(E_h) = h$$

D_0	δ	b_0	γ	K
$[\mathrm{pc}^2\,\mathrm{kyr}^{-1}]$		$[\mathrm{GeV}^{-1}\,\mathrm{kyr}^{-1}]$		$[\mathrm{kyr}^{-1}\,\mathrm{pc}^{-3}\,\mathrm{GeV}^{-1}]$
100	0.4	5×10^{-6}	2.2	1.0×10^{40}

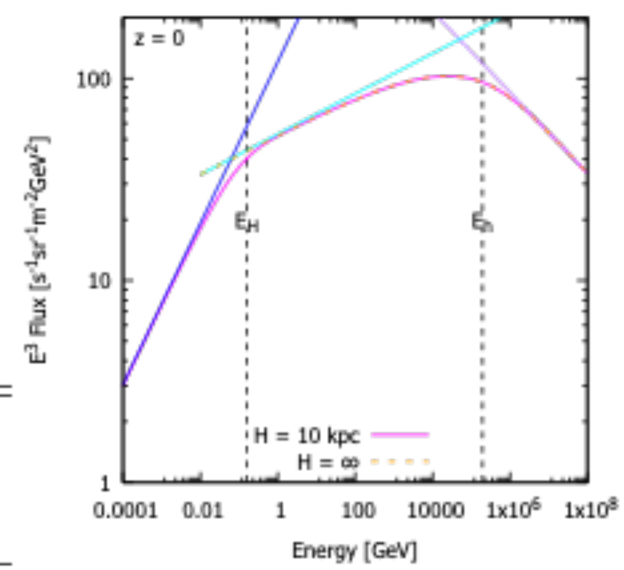

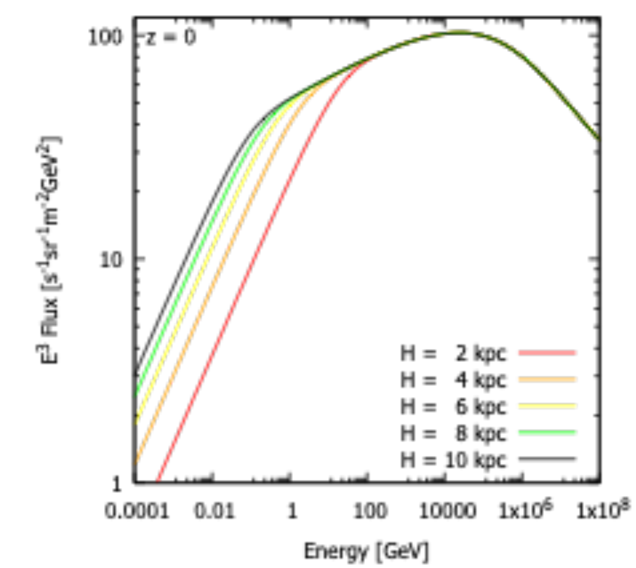

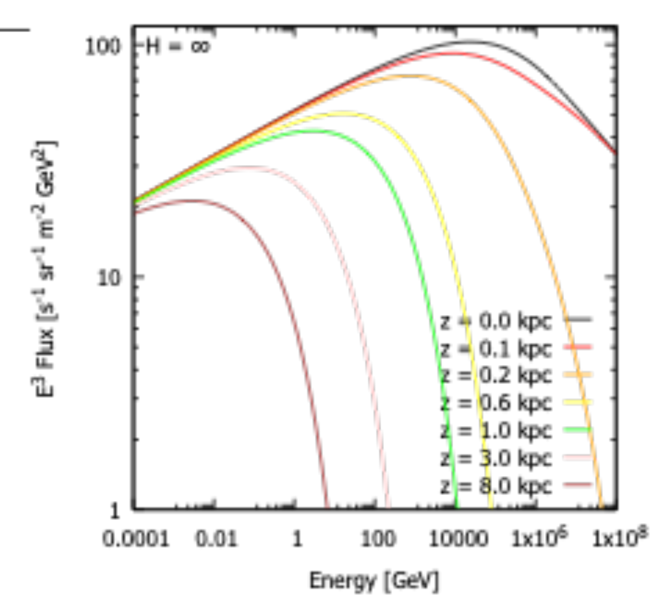

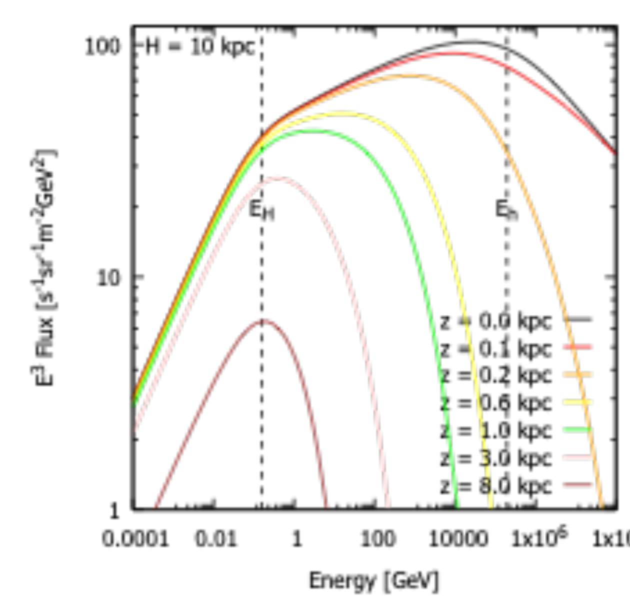

Injection Spectra of Electrons & Positrons

- **Kolmogorov's Spectrum** $\delta = 1/3$
  - **Best-fit Propagation Parameters**

D_0	b_0	h	H
$[\mathrm{pc}^2\,\mathrm{kyr}^{-1}]$	$[\mathrm{GeV}^{-1}\,\mathrm{kyr}^{-1}]$	[pc]	[kpc]
88.386	6.417×10^{-6}	145.164	2.704

  - **Electron Injection Spectrum is double power-law**

$E_H = 4.75\,\mathrm{GeV} \sim E_{br1} = 4.96\,\mathrm{GeV}$ $E_h = 30.7\,\mathrm{TeV}$

- **Electron-Positron Excess**

solar modulation $\phi = 1.273\,\mathrm{GV}$

$C_{e^-}{}^{\dagger}$	γ^1_{e-}	E_{br1}	γ^2_{e-}	E_{br2}	γ^3_{e-}	$C_{e+}{}^{\dagger}$	γ_{e+}	$C^{\dagger}$	γ	E_{cut}
1063	3.347	4.960	3.643	32.355	3.370	163.25	4.048	3.139	2.620	1100

$C^{inj\,\ddagger}_{e-}$	$\gamma^{1,inj}_{e-}$	E^{inj}_{br}	$\gamma^{2,inj}_{e-}$	$C^{inj\,\ddagger}_{e+}$	γ^{inj}_{e+}	$C^{inj\,\ddagger}$	γ^{inj}	E^{inj}_{cut}
6.612×10^{41}	3.059	40.917	2.644	1.053×10^{41}	3.683	1.050×10^{39}	2.040	1555

† with units of $\mathrm{s}^{-1}\,\mathrm{sr}^{-1}\,\mathrm{m}^{-2}\,\mathrm{GeV}^{-1}$.

‡ with units of $\mathrm{kyr}^{-1}\,\mathrm{pc}^{-3}\,\mathrm{GeV}^{-1}$.

Spectra of Electron & Positron

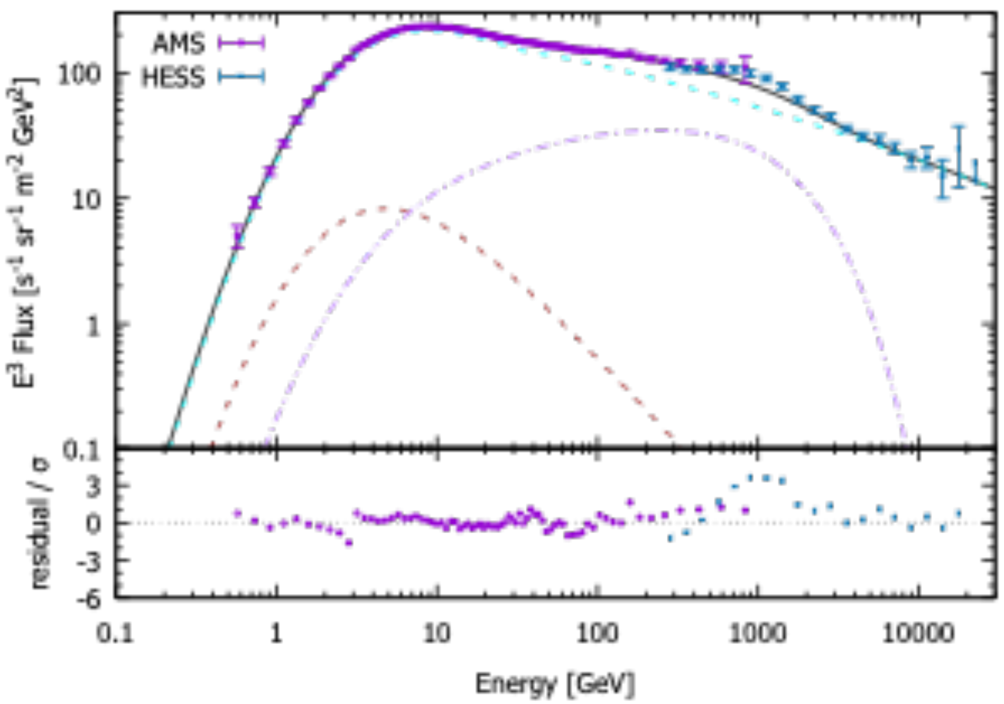

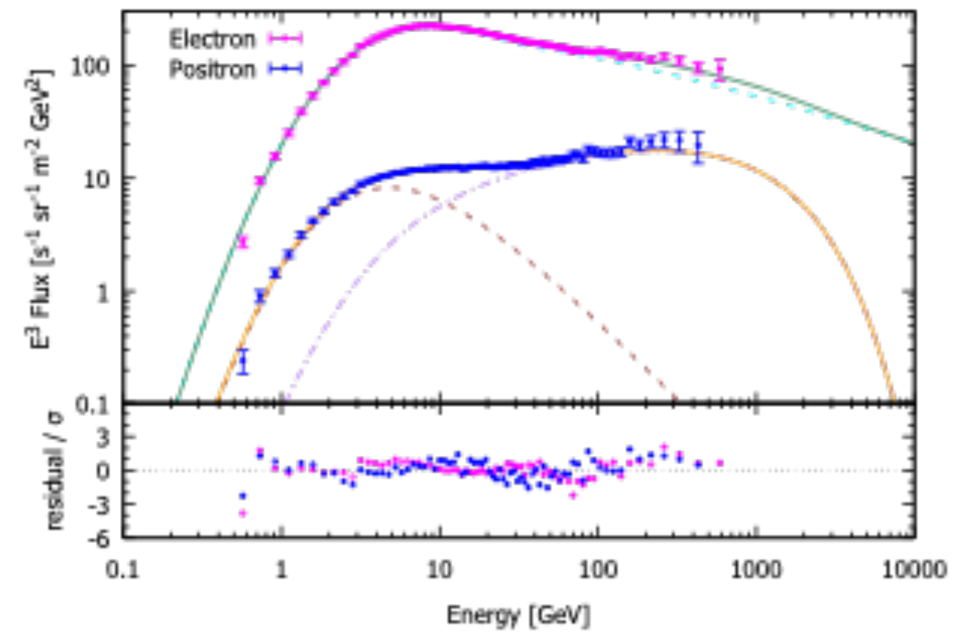

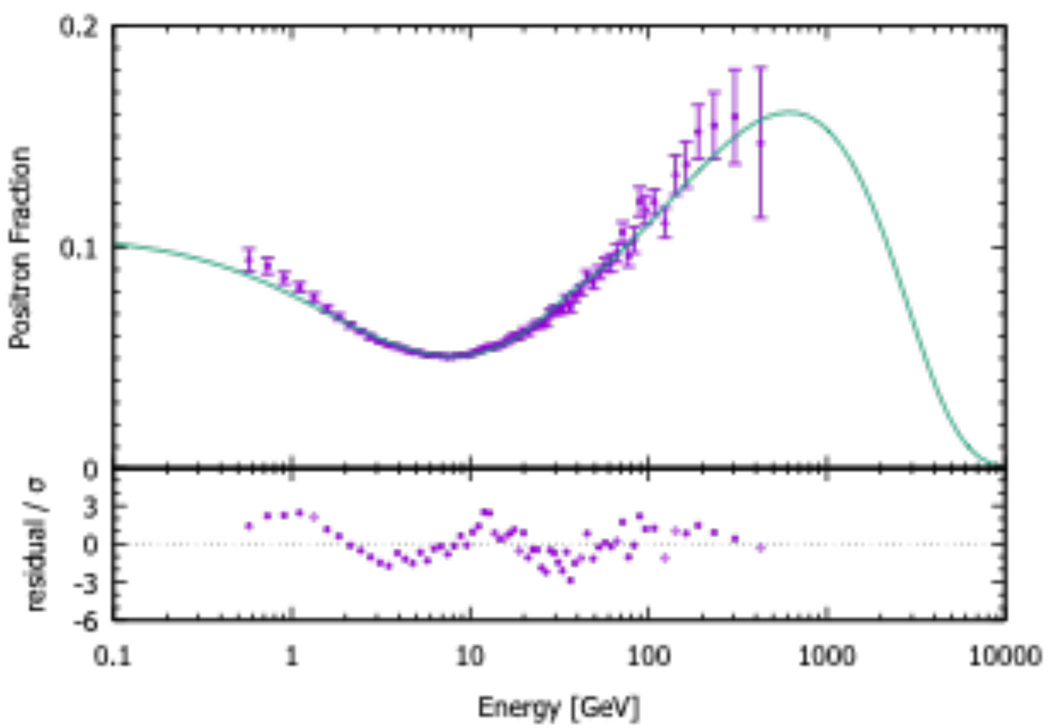

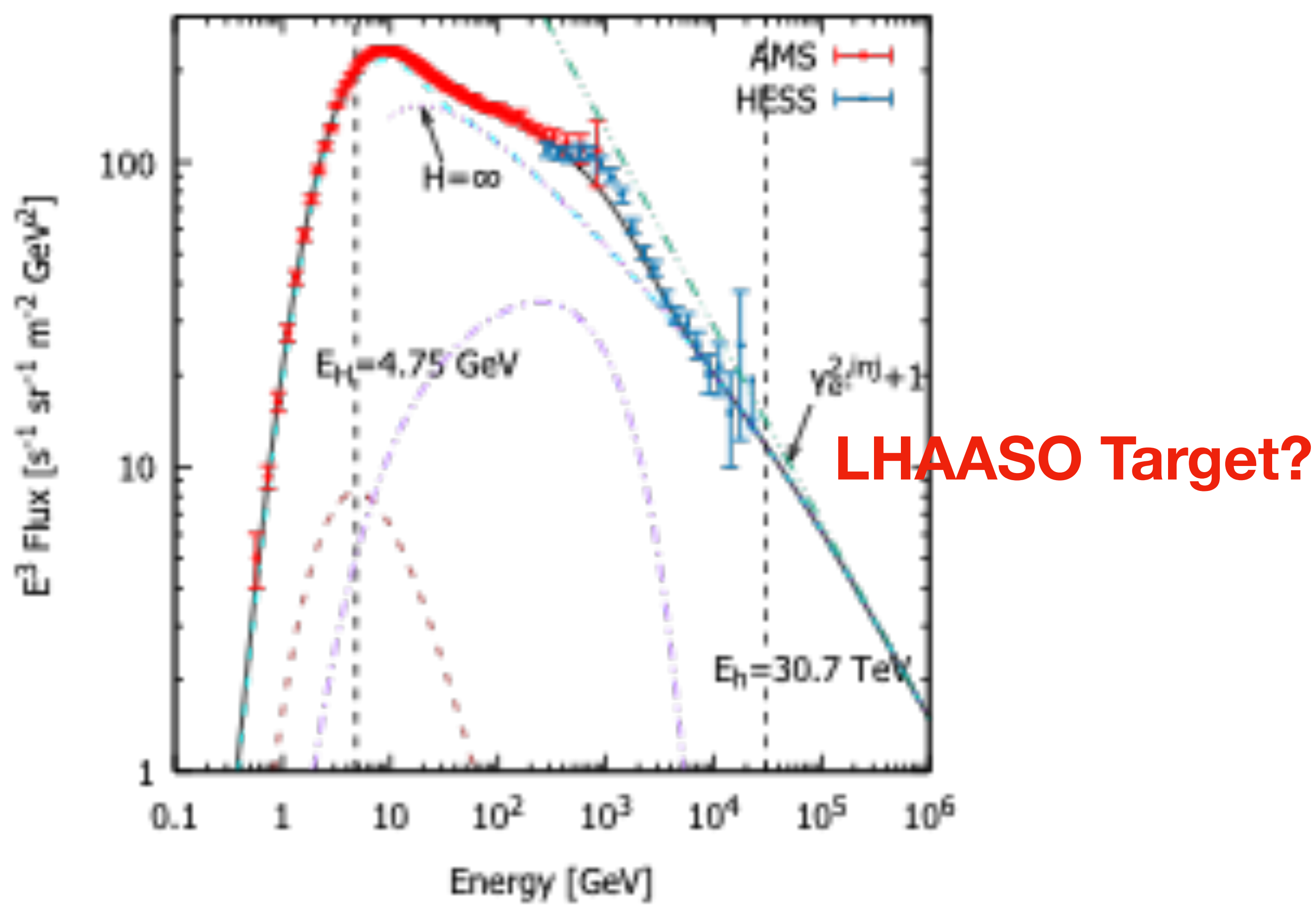

结论

中国科学院紫金山天文台
PURPLE MOUNTAIN OBSERVATORY, CAS

银河系宇宙线起源问题的核心是把宇宙线的观测特征和银河系高能源的观测特征联系起来。

1：如果银河系宇宙线主要来自于超新星遗迹，有迹象表明能量较高的宇宙线主要在遗迹激波演化的早期被加速，而大部分的且能量相对较低的宇宙线在超新星遗迹演化的晚期被加速。

2：年轻超新星遗迹中高能粒子的逃逸概率似乎不依赖于粒子的能量，而在年老遗迹中能谱的高能部分可能从遗迹中完全逃逸。

3：宇宙线正电子很可能主要来源于和脉冲星有关的过程。

4：超新星遗迹中的粒子加速和逃逸模型需要进一步完善以解决银河系宇宙线的起源问题。

5：10TeV以上电子谱测量以及超新星遗迹G150.3+4.5是重要的LHAASO观测对象。

中國科學院紫金山天文台

Purple Mountain Observatory, Chinese Academy of Sciences

Thanks For Your Attention

n=100

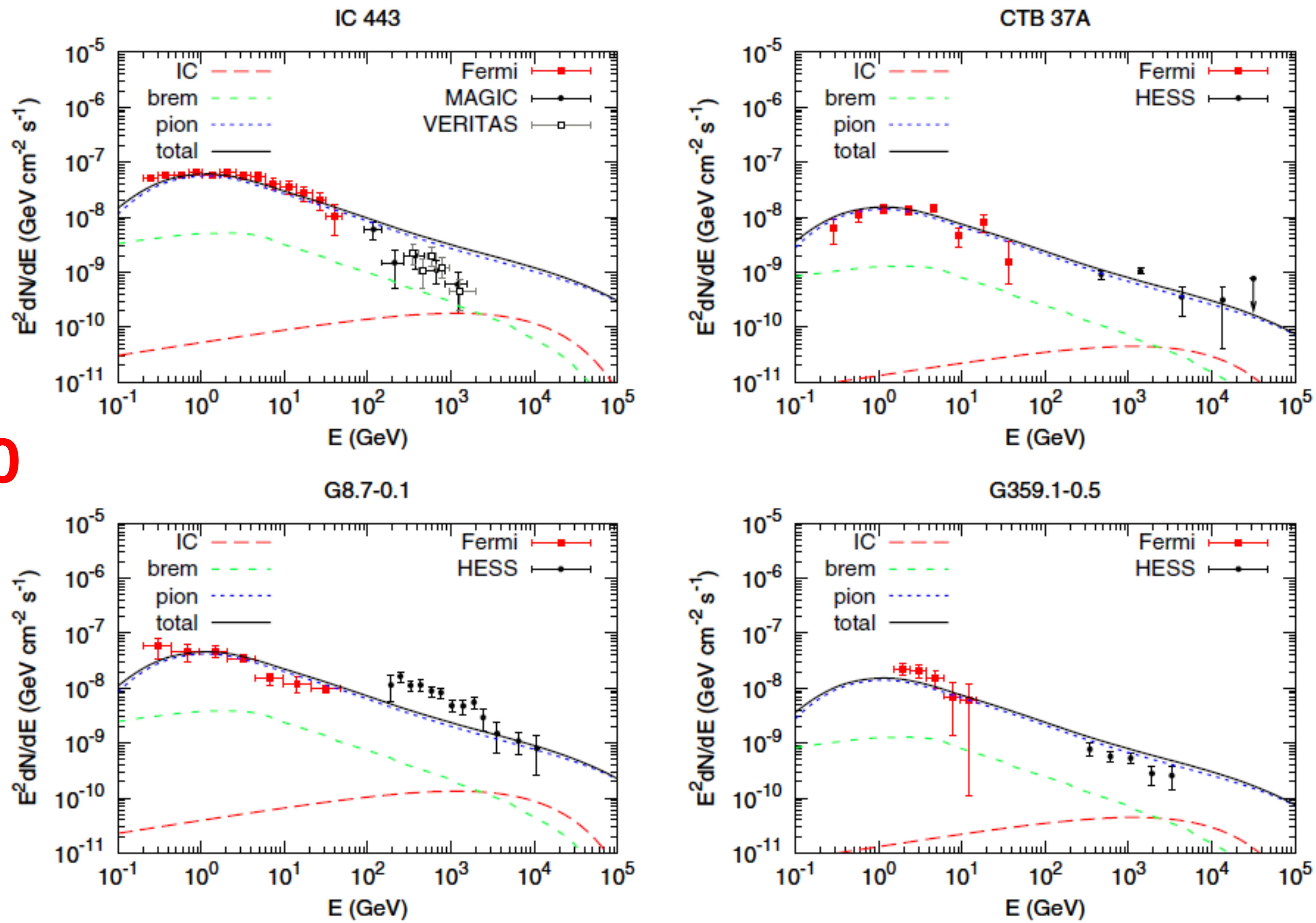

Figure 4. Same as Figure 2, but for SNR–MC interacting systems. The gas density is adopted to be $n = 100\,\mathrm{cm}^{-3}$. References of the observational data—W28: *Fermi* (Abdo et al. 2010a), HESS (Aharonian et al. 2008c); W41: *Fermi* (Mehault et al. 2011), HESS (Mehault et al. 2011); W49B: *Fermi* (Abdo et al. 2010c), HESS (Brun et al. 2011); W51C: *Fermi* (Abdo et al. 2009), HESS (Fiasson et al. 2009), MAGIC (Carmona et al. 2011); IC 443: *Fermi* (Abdo et al. 2010e), MAGIC (Albert et al. 2007a), VERITAS (Acciari et al. 2009); CTB 37A: *Fermi* (Castro & Slane 2010), HESS (Aharonian et al. 2008a); G8.7-0.1: *Fermi* (Ajello et al. 2012), HESS

中国科学院紫金山天文台
PURPLE MOUNTAIN OBSERVATORY, CAS

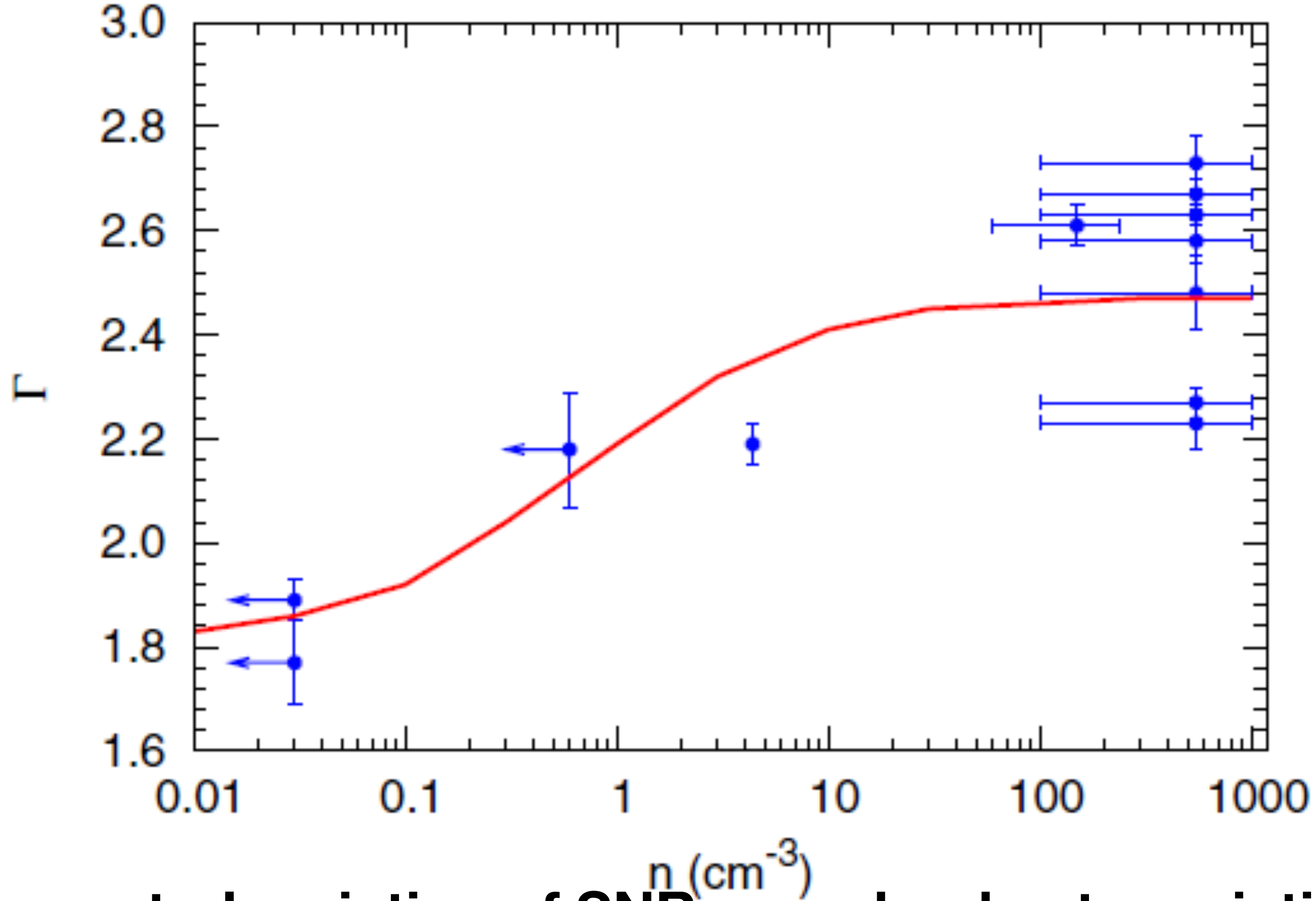

Figure 5. Photon index Γ (between 1 GeV and 1 TeV) vs. the gas density *n* of the 12 SNRs studied in this work. The solid line is the model expected result.

Gamma-ray spectral variation of SNRs may be due to variation in density of the surrounding environment.

These results can be considered as evidence for the SNR origin of Galactic cosmic rays.

Results

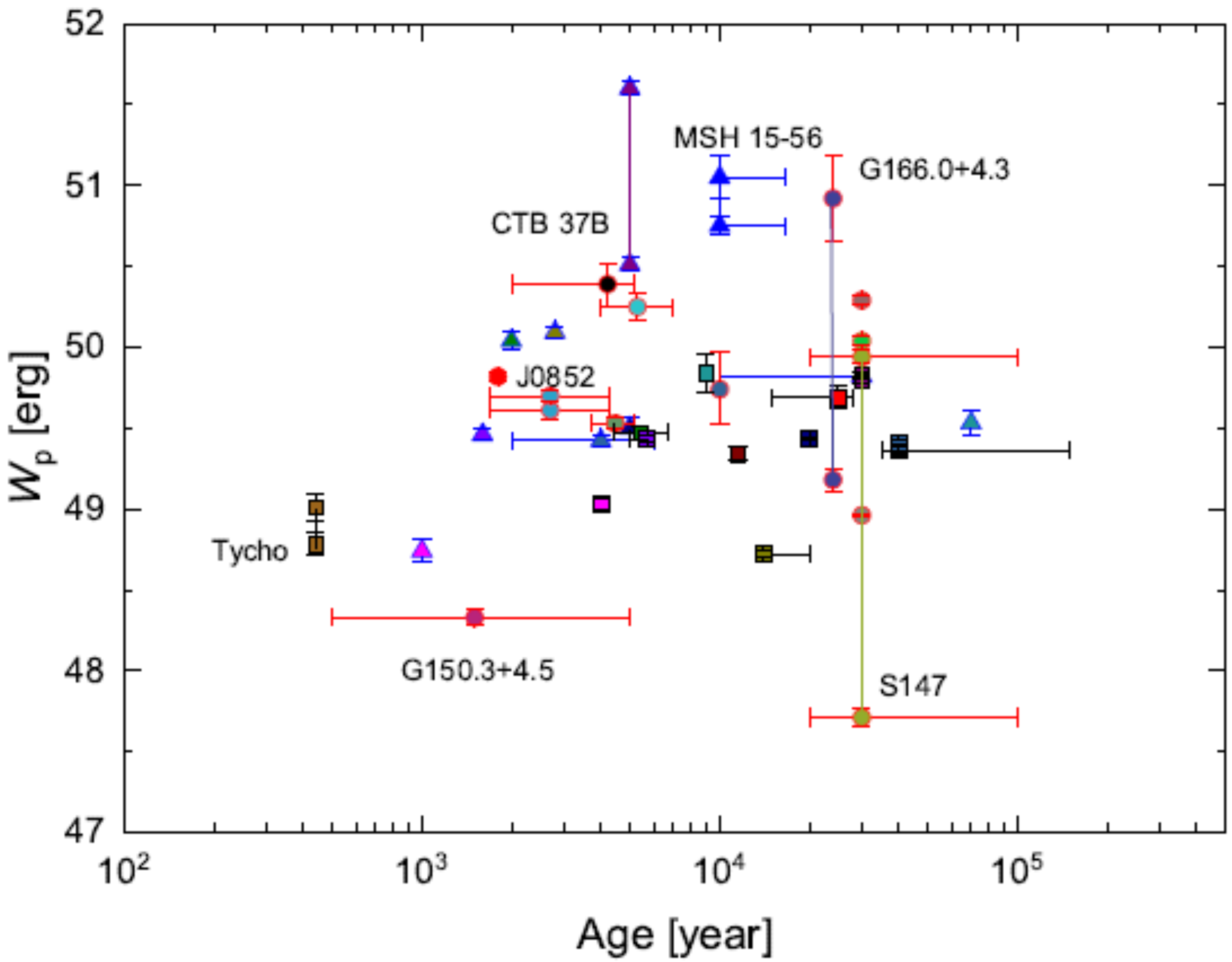

The total energy of particles for most of SNRs are greater than erg which can be regarded as the lower limit of the cosmic rays produced by SNRs, and also supports that SNRs are the sources of Galactic cosmic rays.

Results

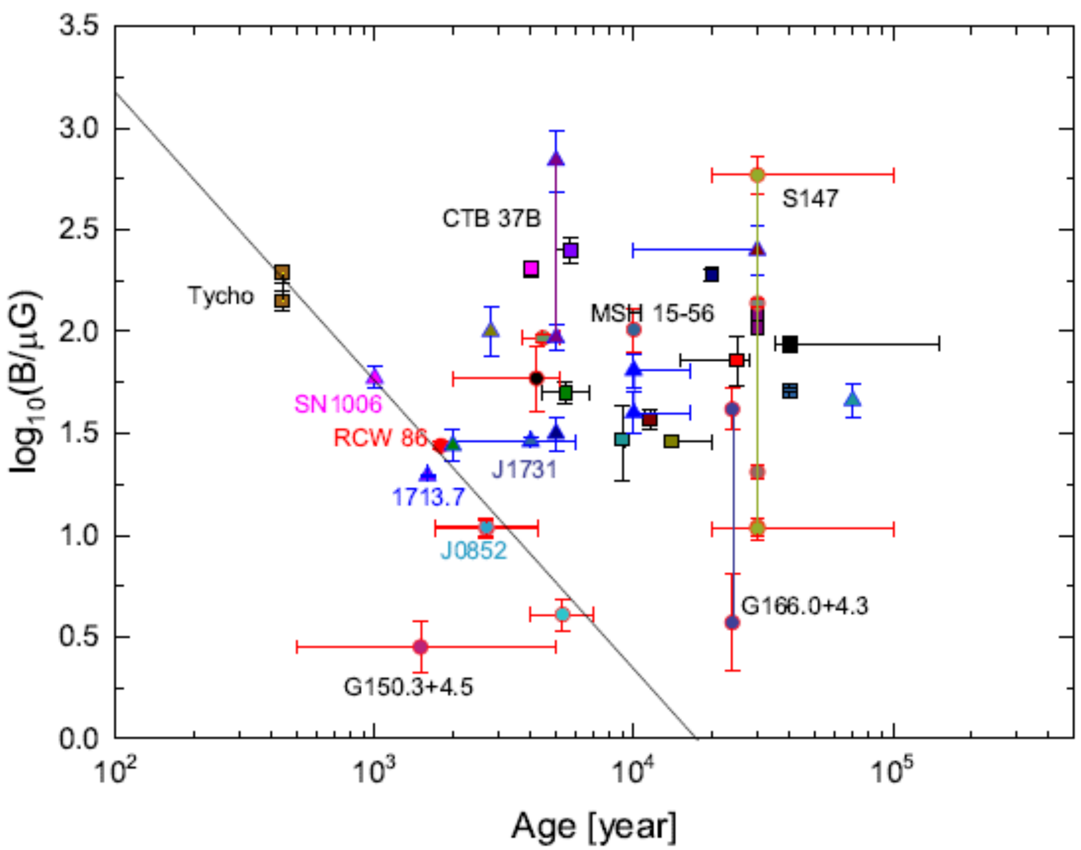

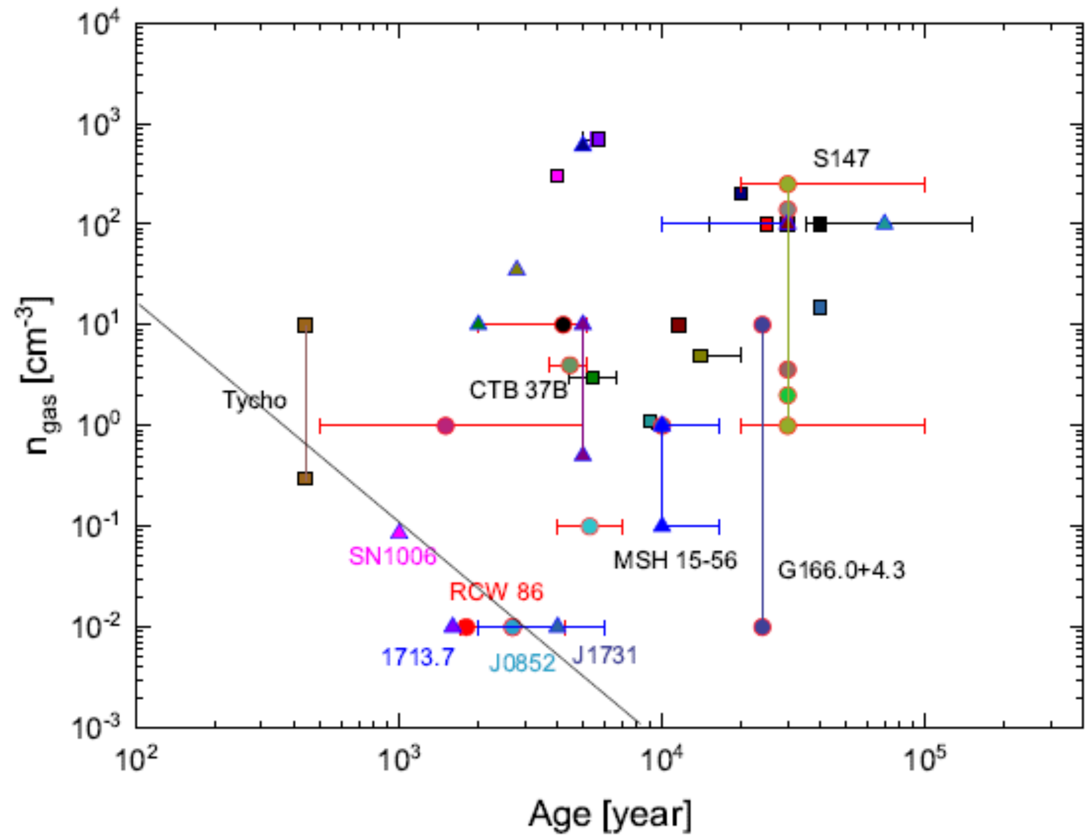

These two figures respectively show that the relationship between the magnetic field, the gas density and the age of SNRs. The results show there are no correlation between them, but an anti-correlation may be existence for several young shell-type SNRs, consistent with evolution in wind bubbles.

Results and discussion

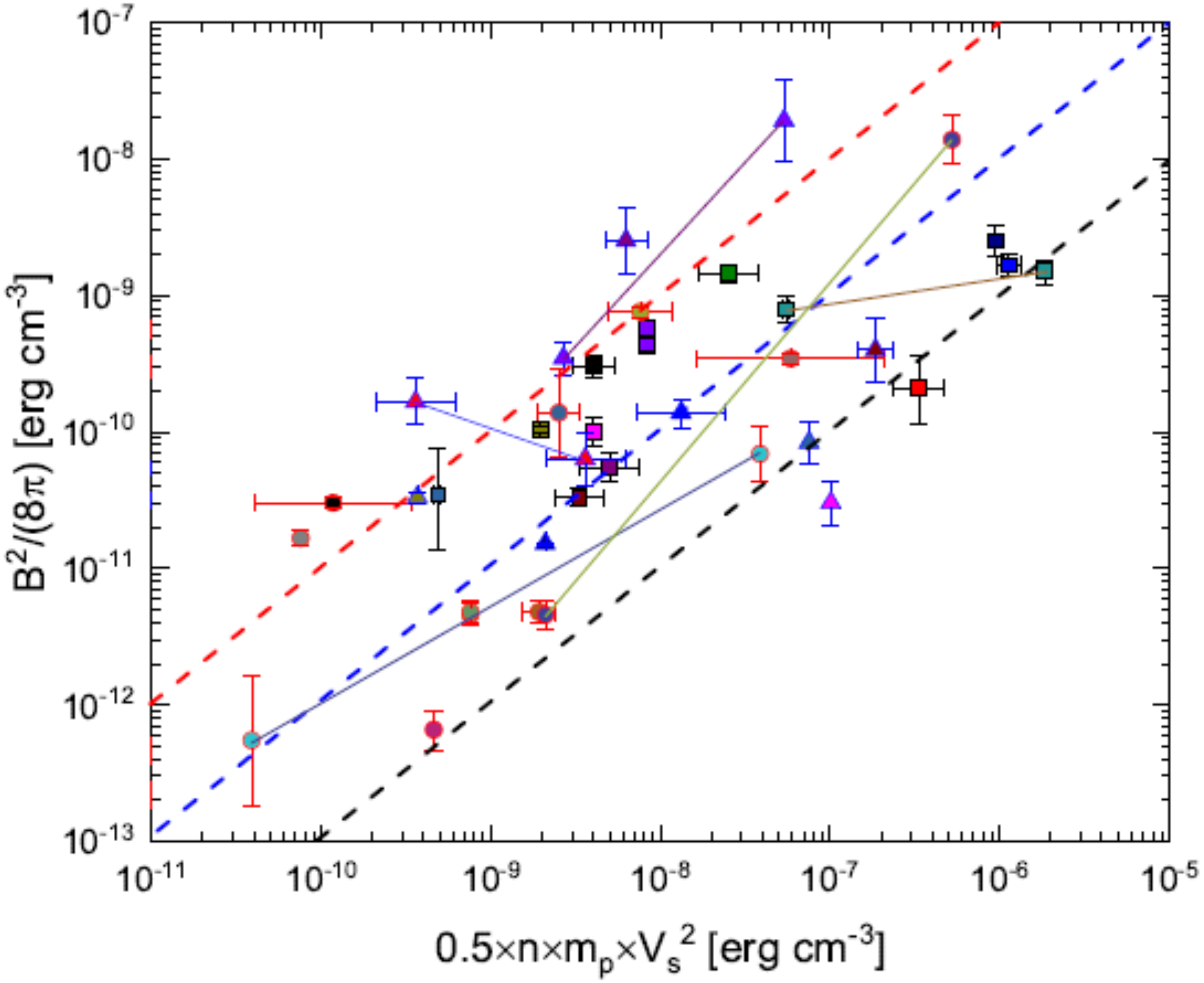

Results

中国科学院紫金山天文台
PURPLE MOUNTAIN OBSERVATORY, CAS

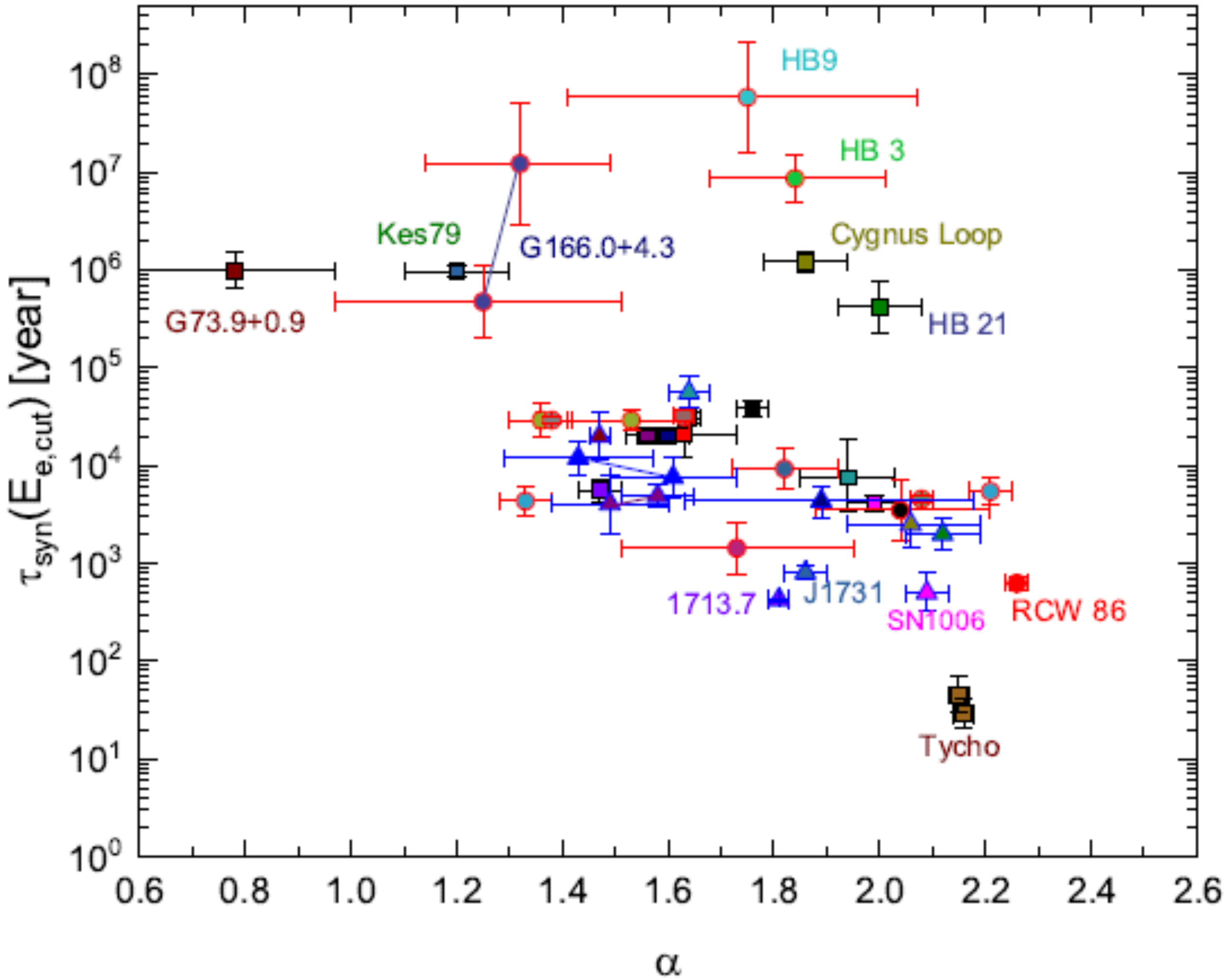

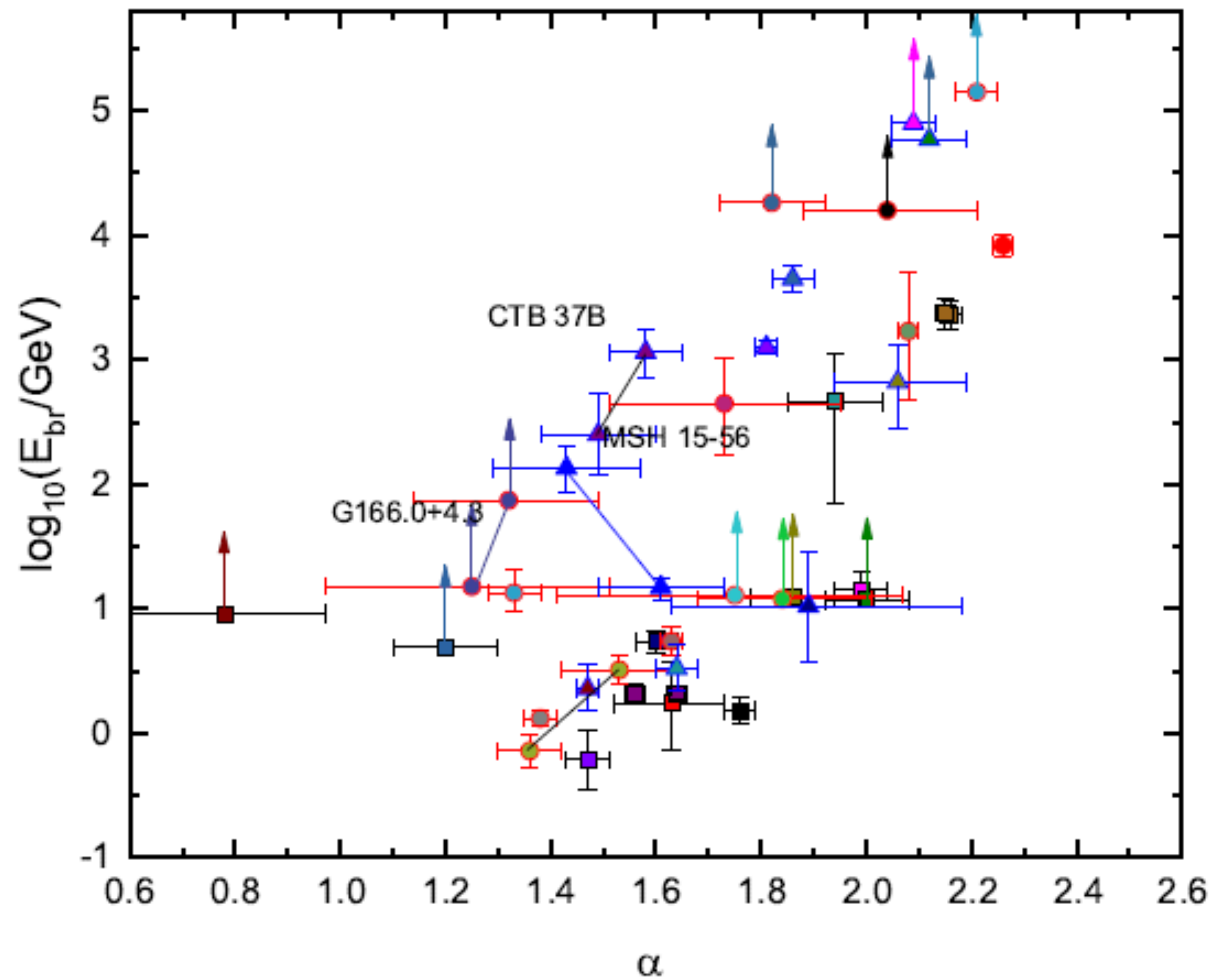

Discussion

(Possible relation between Particles and CRs spectrum)

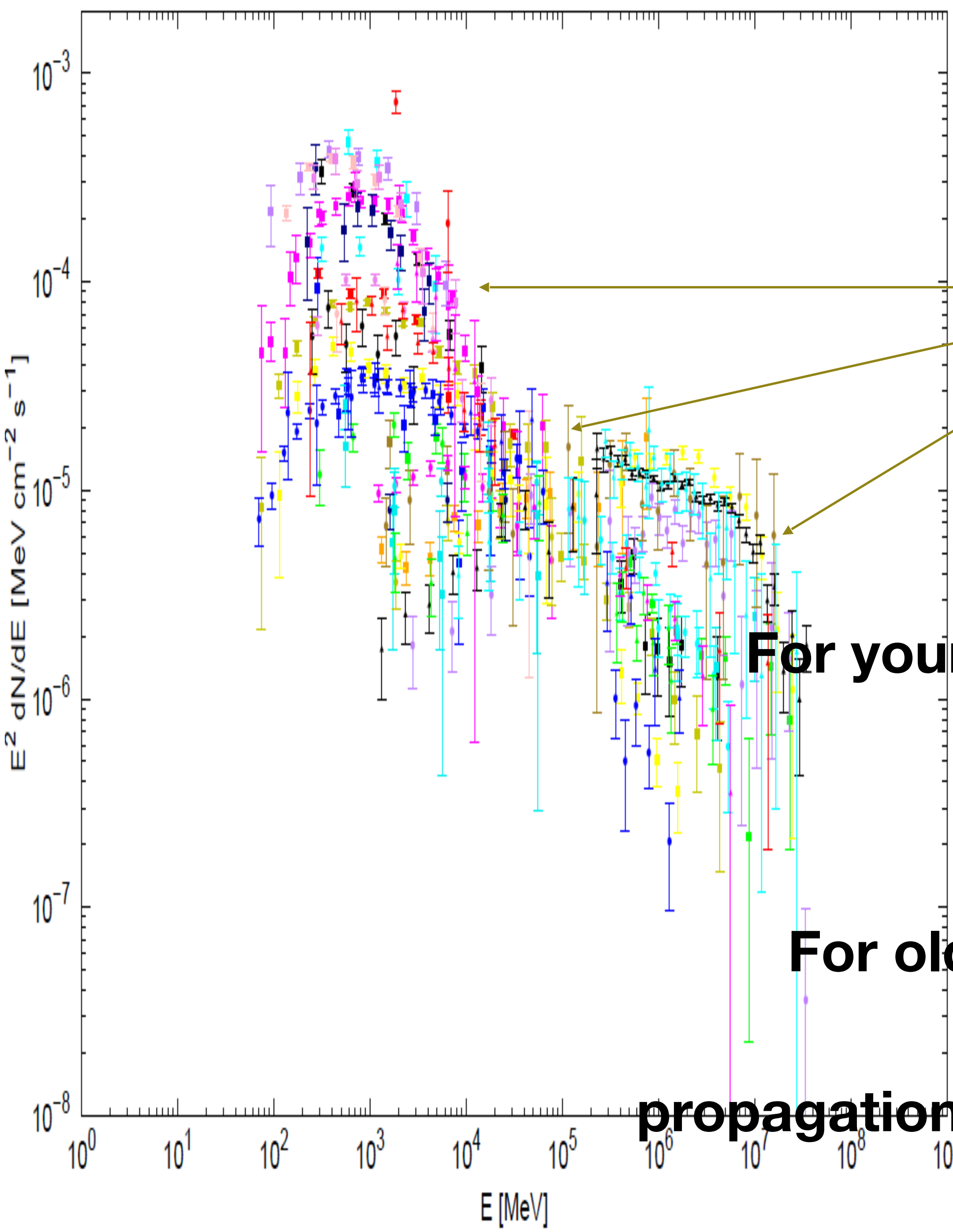

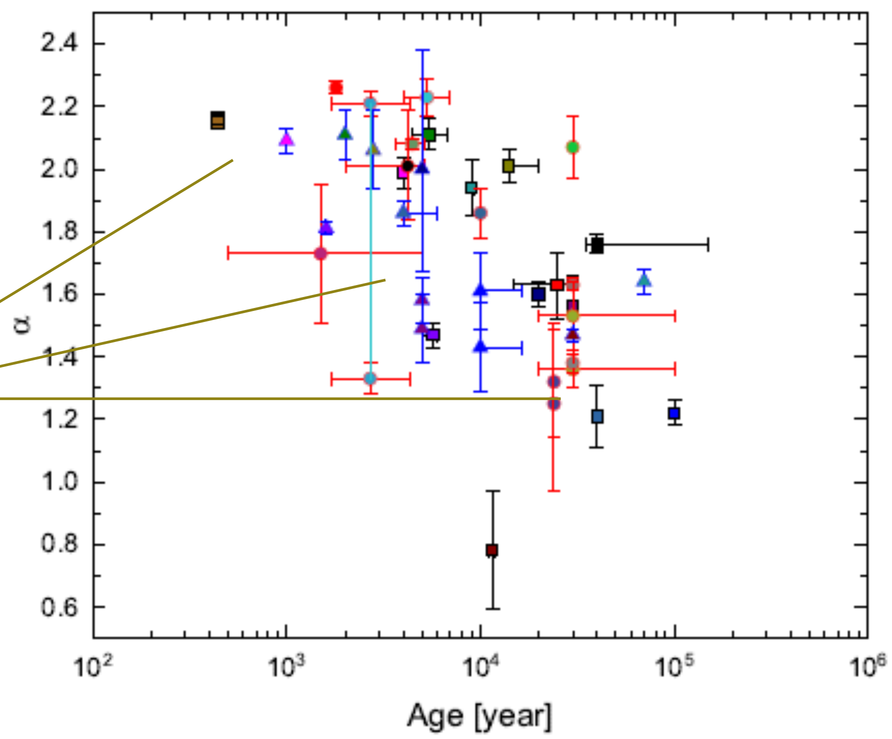

For young SNRs:

For old SNRs:

propagation effect 0.3-0.6

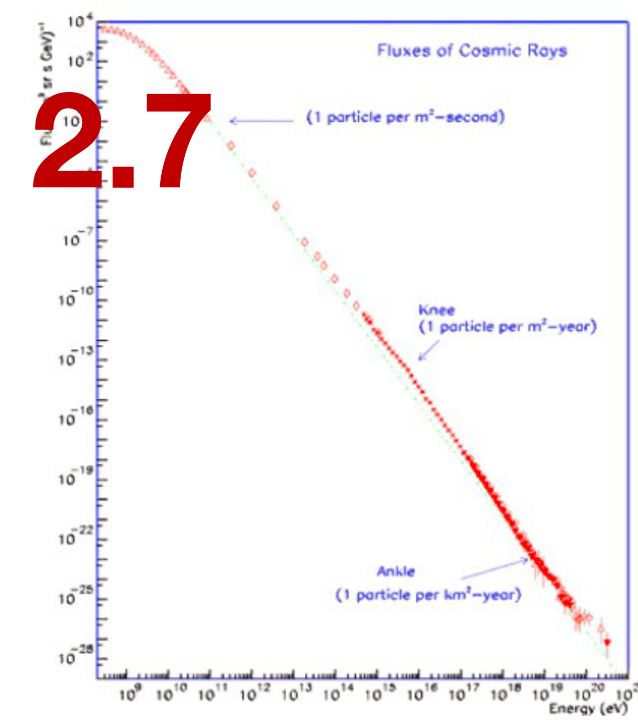

2.7